

PARAMETRIC STUDY ON THE DESIGN OF BAFFLE FOR THREE-
DIMENSIONAL TURNING DIFFUSER

NUR HAZIRAH BINTI NOH @ SETH

A thesis submitted in
fulfillment of the requirement for the award of the
Doctor of Philosophy

Faculty of Mechanical and Manufacturing Engineering
University Tun Hussein Onn Malaysia

NOVEMBER 2016

To my husband Mohd. Salehin Hj. Mazelan,
My better half,
Who helped me through thick and thin in this entire adventure

To my son Muhammad Nur Uwais Mohd Salehin,
My heaven and earth,
Who gave me strength to complete this thesis

To my heartbeat,
Zaiton Hj. Hashim, Hjh. Saleha Hj. Jaman and Hj. Mazelan Hj. Yusoff
Who always pray for my success

Last and foremost,

To my beloved father Allahyarham Noh@Seth Hj. Ismail,
My inspiration

ACKNOWLEDGEMENT

I would like to express my sincere appreciation to my supervisor, Dr. Norasikin Mat Isa for all the guidance and support throughout the entire duration in completing this thesis. Thank you so much.

Credit should also be given to UTHM Aerodynamic Lab technician, Mr. Zainal for his cooperation and Dr. Normayati who taught me on hands on practical of PIV before running the experiment myself. Appreciation also goes to other PhD candidatures who keep on inspiring me; Zila, Najwa, Rasidi, Kak Syikin, Fatimah, Mun and many others. Thanks for the advices and help along the journey. May success be with all of us, all the time, Amiin.

This emotional journey would not be complete without the constant advices and helps from the best of friend; Ayong, Iza, Yuyun, Mira, Shahed, Wani, Nani, Efa, Jah, Sha, Zura and Ecah. Thank you for the constant instant messages regardless of the topic and always brings the best out of me. Knowing all of you is a blessed, but having all of you by my side throughout these years is always a miracle.

ABSTRACT

Secondary flow developed in the inner wall region within a turning diffuser will reduce its performance particularly in terms of both pressure recovery (C_p) and flow uniformity (σ_u). Introduction of baffle is effective in reducing separated flow in turning diffuser, hence enhance its performance. Therefore, flow structure in three-dimensional turning diffuser with baffle was studied and the subsequent impacts towards turning diffuser performance was observed. A parametric study was also conducted on the preliminary design of airfoil in determining the most optimum baffle design. An experiment was conducted with inflow Reynolds number (Re_{in}) that was varied between $4.527\text{E}+04$ and $1.263\text{E}+05$. As measured by using pressure tapping that was connected to a digital Manometer, a pressure recovery of $C_p=0.341$ was obtained when the system was operated at Reynolds number $Re_{in}=1.263\text{E}+05$. This result had shown an improvement of up to 43% compared to the previous study with pressure recovery $C_p=0.194$. Similarly, the flow uniformity which was measured by using Particle Image Velocimetry (PIV) had improved up to 33% at $Re_{in}=9.950\text{E}+04$ with $\sigma_u=3.09$ as compared to the previous study, where $\sigma_u=4.64$. A parametric study on the preliminary baffle design was also simulated using ANSYS Fluent, which had been verified and validated according to experimental data. The parametric study involved varying several parameters such as type of baffle, the angle of attack, AOA, thickness to chord ratio [t/c (%)], camber to chord ratio [f/c (%)], and chord length [c (cm)]. Simulations of various 23 designs with combination of several parameter changes had discovered an optimum design of airfoil with AOA= 16° , $t/c = 7.658\%$, $f/c = 7\%$ and chord length, $c = 5$ cm. In comparison to the preliminary airfoil design, that optimum design for the three-dimensional turning diffuser had achieved 7.202% and 6.164% performance improvement in terms of flow uniformity and pressure recovery, respectively.

ABSTRAK

Aliran menengah yang terbentuk di rantau dinding dalam penyerap getaran akan menyebabkan prestasi menurun dari segi liputan tekanan (C_p) dan keseragaman aliran (σ_u). Pengenalan sesekat dapat membantu dalam mengurangkan aliran menengah dan memperbaiki prestasi penyerap getaran. Oleh itu, struktur aliran dalam penyerap getaran 3 dimensi dengan sesekat dikaji dan kesannya terhadap prestasi penyerap getaran dsiasat. Eksperimen ke atas sesekat bentuk aerofoil permulaan yang diuji dengan nombor alir masuk Reynolds (Re_{in}) di antara $4.527E+04 - 1.263E+05$ telah dijalankan, menghasilkan liputan tekanan $C_p=0.341$, dimana ianya diukur dengan menggunakan tekanan menoreh yang disambung ke Manometer digital, dicatatkan apabila sistem beroperasi dengan nombor Reynolds paling tinggi yang iaitu $Re_{in}=1.263E+05$. Keputusan ini menunjukkan peningkatan sehingga 43% daripada kajian lepas iaitu $C_p=0.194$ pada nombor Reynolds yang sama. Keseragaman aliran, yang diukur menggunakan *Particle Image Velocimetry (PIV)* juga menunjukkan peningkatan sebanyak 33% daripada kajian lepas pada $Re_{in}=9.950E+04$ iaitu $\sigma_u=3.09$ jika dibandingkan dengan kajian lepas iaitu $\sigma_u=4.64$. Kajian parametrik ke atas reka bentuk permulaan sesekat dilakukan menggunakan simulasi pada ANSYS Fluent, dimana keputusannya disahkan menggunakan nilai kajian dari eksperimen. Kajian parametrik merangkumi menukar jenis sesekat, sudut serang (AOA), nisbah tebal perentas, $t/c(\%)$, kamber nisbah perentas, $f/c(\%)$ dan panjang perentas, $c(cm)$. Simulasi ke atas 23 rekaan dengan pelbagai perubahan parameter menghasilkan reka bentuk optimum iaitu $AOA=16^\circ$, $t/c=7.658\%$, $f/c=7\%$ dan panjang perentas, $c=5$ cm. Reka bentuk optimum menyebabkan peningkatan prestasi penyerap getaran 3 dimensi sebanyak 7.202% dari segi keseragaman aliran jika dibandingkan dengan aerofoil permulaan dan peningkatan sebanyak 6.164% dari segi liputan tekanan.

CONTENTS

TITLE	i
DECLARATION	ii
DEDICATION	iii
ACKNOWLEDGEMENT	iv
ABSTRACT	v
ABSTRAK	vi
CONTENTS	vii
LIST OF TABLES	xi
LIST OF FIGURES	xiv
LIST OF SYMBOLS	xxii
LIST OF ABBREVIATIONS	xxiv
LIST OF APPENDICES	xxvi
CHAPTER 1 INTRODUCTION	1
1.1 Research background	4
1.2 Problem Statement	6
1.3 Objectives of study	7
1.4 Scope of study	7
1.5 Significance of study	8
1.6 Thesis outline	9

CHAPTER 2	LITERATURE REVIEW	11
2.1	Diffuser applications and turning diffuser theoretical background	12
2.2	Experimental rig development on low subsonic wind tunnel feature	16
2.3	Various baffles design	25
2.4	PIV instrumentations	33
2.5	Numerical analysis solutions	35
CHAPTER 3	METHODOLOGY: EXPERIMENTAL APPROACH	41
3.1	Experimental method	42
3.1.1	Experimental setup	42
3.1.2	Centrifugal blower	43
3.1.3	Settling chamber and screens	45
3.1.4	Contraction cone	46
3.1.5	Rectangular duct	47
3.1.6	Turning diffuser with airfoil baffle	48
3.1.7	Initial condition measurement	50
3.1.8	Pressure recovery and efficiency measurement	54
3.2	PIV measurement and instrumentation	57
3.2.1	2D PIV setup	59
3.2.2	3D PIV setup	60
3.2.3	Tracer particle seeding	62
3.2.4	Illumination	64
3.2.5	Photographing	66
3.2.6	Image processing	70
CHAPTER 4	METHODOLOGY: NUMERICAL METHOD	73
4.1	Description of the whole system	74
4.2	Mathematical model	74
4.3	Computational domain	76
4.4	Domain discretization	77
4.5	Boundary and operating conditions	80

4.6	Solver and solution algorithm	82
4.7	Convergence criteria	84
CHAPTER 5	EXPERIMENTAL DATA ANALYSIS	89
5.1	Design of baffles	90
5.2	Measurement of initial condition	92
5.3	Measurement of static pressure recovery	93
5.4	Flow structure in three-dimensional turning diffuser	95
5.5	Outlet flow uniformity, σ_{out} measurement	111
5.6	Turning diffuser efficiency	120
CHAPTER 6	NUMERICAL DATA ANALYSIS	123
6.1	Numerical work on 2D turning diffuser with baffles	123
6.1.1	Computational domain	124
6.1.2	Domain discretization	124
6.1.3	Flow structure in two-dimensional turning diffuser with baffles	126
6.2	Numerical work on 3D turning diffuser with baffle	130
6.2.1	Computational domain	130
6.2.2	Domain discretization	131
6.2.3	Flow structure in the three-dimensional turning diffuser with baffle	132
6.2.4	Outlet plane velocity contour	141
CHAPTER 7	VERIFICATION AND VALIDATION	143
7.1	Verification of the two-dimensional turning diffuser solutions	144
7.1.1	Grid independence study on two-dimensional turning diffuser with baffles	144
7.1.2	Turbulence model test on two-dimensional turning diffuser with baffles	147
7.1.3	Numerical scheme test on two-dimensional turning diffuser with baffles	149
7.1.4	Convergence criteria test on two-dimensional turning diffuser with baffles	150
7.2	Validation of the two-dimensional turning diffuser with baffles	152
7.3	Verification of the three-dimensional turning diffuser solutions	155

7.3.1	Grid independence study on three-dimensional turning diffuser with baffle	156
7.3.2	Turbulence model test on three-dimensional turning diffuser with baffle	159
7.3.3	Numerical scheme test on three-dimensional turning diffuser with baffle	160
7.3.4	Convergence criteria test on three-dimensional turning diffuser with baffle	161
7.4	Validation on three-dimensional turning diffuser with baffle solutions	163
CHAPTER 8 CFD STUDY ON VARIOUS BAFFLE DESIGNS		167
8.1	Parametric study on the design of baffle	169
8.2	Parametric study on airfoil angle of attack (AOA)	184
8.3	Parametric study on thickness to chord ratio, t/c (%)	198
8.4	Parametric study on camber to chord ratio, f/c (%)	203
8.5	Parametric study in chord length, c (cm)	209
CHAPTER 9 CONCLUSIONS AND FUTURE WORK		215
9.1	Conclusions	215
9.2	Contributions	217
9.3	Recommendations on future work	218
REFERENCES		219
LIST OF PUBLICATIONS		230
APPENDICES		231

LIST OF TABLES

2.1	Pressure loss coefficient (K) (Nordin et al., 2011)	18
2.2	C_p measured for each Re_{in} tested and verification of PIV results for two-dimensional turning diffuser (Nordin et al., 2014a)	20
2.3	Result comparison between Noh@Seth et al. (2013) and Nordin et al. (2014a) for both C_p and σ_{out}	22
2.4	Mean outlet velocity, V_{out} and flow uniformity comparison, σ_{out} (Nordin et al., 2014a)	24
2.5	Pressure recovery, C_p comparison (Nordin et al., 2014a)	24
3.1	Input parameters for centrifugal blower	45
4.1	ANSYS Fluent input parameters	86
5.1	Preliminary airfoil parameters	91
5.2	Measurement of inlet conditions	93
5.3	Measurement of static P_i and P_o	93
5.4	Comparison of C_p	94
5.5	Selection of Δt	96
5.6	U_{max} comparison for validation of Δt . Optimum Δt is marked with (*)	97
5.7	U_o extracted along Line 1 for the selected Δt	98
5.8	Comparison of U_{in} measurement	102
5.9	V_o comparison for validation of Δt . Optimum Δt were marked with (*)	113
5.10	V_o extracted at outlet plane for selected Δt	114
5.11	V_{out} (m/s) comparison with previous study	116
5.12	Calculated value of diffuser efficiency, η for the present study	121
5.13	Calculated value of diffuser efficiency, η for Nordin et al. (2014a)	121

6.1	Calculation of first layer thickness for 2-dimesional turning diffuser with baffle	125
6.2	Turbulence intensity measurement at both inlet and outlet	126
6.3	Calculation of first layer thickness for three-dimensional turning diffuser with baffle	131
7.1	Three types of meshes tested for grid independence study	146
7.2	Numerical scheme CPU hours needed to reach convergence	149
7.3	Convergence criteria CPU hours needed to reach convergence	151
7.4	Comparison of P_i	152
7.5	Comparison of P_o	152
7.6	Comparison of C_p	153
7.7	Comparison of V_{out}	153
7.8	Experimental value of the two-dimensional turning diffuser with baffle efficiency, η	154
7.9	CFD value of the two-dimensional turning diffuser with baffle efficiency, η	154
7.10	Comparison of η	155
7.11	Three types of meshes tested in grid independence study	158
7.12	Numerical scheme CPU hours needed to reach convergence	160
7.13	Convergence criteria CPU hours needed to reach convergence	162
7.14	Comparison of P_i	163
7.15	Comparison of P_o	164
7.16	Comparison of C_p	164
7.17	Comparison of V_{out}	165
7.18	CFD value of three-dimensional turning diffuser with baffle efficiency, η	165
7.19	Comparison of η	165
8.1	Design parameters changes in determining optimum design of baffle	168
8.2	Static pressure comparison between flat plate and airfoil baffle	171
8.3	C_p comparison between flat plate and airfoil baffle	171
8.4	Mean outlet velocity, V_{out} comparison between flat plate and airfoil	172
8.5	σ_{out} comparison between both designs of baffle	172
8.6	η comparison between both designs of baffle	173

8.7	Turning diffuser performance comparison for airfoil with various AOA tested	185
8.8	Turning diffuser efficiency, η comparison for airfoil with various AOA tested	186
8.9	Drag coefficient measured for airfoil with various AOA tested	186
8.10	Turning diffuser performance for each airfoil with various AOA tested	194
8.11	Turning diffuser efficiency, η comparison for airfoils with various AOA tested	194
8.12	Drag coefficient, C_d measured for each AOA	195
8.13	Airfoil characteristics tested	198
8.14	Turning diffuser performance for each airfoil tested	199
8.15	Turning diffuser efficiency, η comparison for each t/c tested	200
8.16	Drag coefficient measured for each airfoil	200
8.17	Airfoil tested in changes of f/c	204
8.18	Turning diffuser performance for each airfoil tested	205
8.19	Turning diffuser efficiency, η comparison for each f/c tested	205
8.20	Drag coefficient measured for each airfoil	206
8.21	Airfoil properties tested in changes in chord length, c	209
8.22	Turning diffuser performance for each airfoil tested	210
8.23	Turning diffuser efficiency, η comparison for each c tested	210
8.24	Drag coefficient measured for each airfoil	211
8.25	Performance comparison between base airfoil and optimum airfoil	214
9.1	Design parameters of the optimum baffle	216

LIST OF FIGURES

1.1	Schematic diagram of experimental circulating fluidised bed including diffuser (Schut et al., 2000)	2
1.2	Test rig measurement of diffuser's pressure loss coefficient in HVAC free discharge duct system (Gan & Riffat, 1996)	3
1.3	Closed loop subsonic wind tunnel detailed computer-aided design CAD model (Calautit et al., 2014)	3
1.4	Design of the two-dimensional turning diffuser (Nordin et al., 2012)	5
1.5	Design of the three-dimensional turning diffuser (Nordin et al., 2012)	5
2.1	Two different positions of diffuser in the riser; (a) 550 cm below the exit and (b) 1050 cm below the exit (Schut et al., 2000)	12
2.2	Bend-diffuser combination with short spacer shows highly distorted flow at diffuser exit for both studies by; (a) Gan & Riffat (1996), (b) El-Askary & Nasr (2009)	13
2.3	(a) Contours of velocity magnitude for wind tunnel before and (b) after installation of guide vanes (Calautit et al., 2014)	15
2.4	Location chosen for measurement; S1, S2, S3 (Nordin et al., 2011)	17
2.5	Two planes selected for each location measurement (Nordin et al., 2011)	17
2.6	Rig development of low subsonic wind tunnel. All dimensions in cm. (Nordin et al., 2013)	19
2.7	(a) Five points location at inlet for measurements of fully developed flow and (b) velocity profile measured using Pitot static probe (Nordin et al., 2014b)	20
2.8	Flat plate baffle designed by Noh@Seth et al. (2013). All dimensions in cm.	21

2.9	Outlet velocity contour and vector comparison between (a) Nordin et al. (2014a) and (b) Noh@Seth et al. (2013). Red box indicates inner wall region.	23
2.10	Schematic diagram of experimental setup using diffusing bend (Friedman & Westphal, 1952)	25
2.11	Sketch showing airfoil location and cascade end condition (Friedman & Westphal, 1952)	26
2.12	Airfoil profile (Friedman & Westphal, 1952)	26
2.13	Computer velocity vectors on sharp 180° bend duct (a) without guide vane, and (b) with one guide vane (Modi & Jayanti, 2004)	27
2.14	The cascade vane geometry used by Lindgren et al. (1998); d =spacing between vanes, c =chord length, h_0 =spacing between vanes perpendicular to outflow direction, h_I =spacing between vanes perpendicular to inflow direction	28
2.15	Solid line guide vane is the optimised guide vane for non-expanding corners. Dashed line is the new vane optimised for expanding corners. (Lindgren & Johansson, 2002)	29
2.16	Mean velocity contour around airfoil for (a) AOA=0°, (b) AOA=6° and (c) AOA=15°. RA=reattachment, S=separation. (Nakano et al., 2007)	30
2.17	Geometry of cascades (Schreiber et al., 2004)	31
2.18	Comparison of leading edge geometry (Schreiber et al., 2004)	31
2.19	Schematic diagram of the turning vanes in Mathew (2006)	33
2.20	Schematic diagram of stereoscopic PIV setup taken from Prasad (2000)	34
2.21	Validation process (Standard A.I.A.A, 1999)	36
2.22	Verification process (Standard A.I.A.A, 1999)	36
2.23	(a) Full scale of entire closed circuit wind tunnel; (b) Test section for wind tunnel with inlet and outlet boundary condition (Moonen et al., 2006).	37
2.24	Instantaneous velocity field obtained by LES (Jakirlić et al., 2010)	39
3.1	Schematic diagram of the experimental setup (Nordin et al., 2013)	43
3.2	Actual diagram of the experimental setup consists of; (a) centrifugal blower, settling chamber with screens and	

contraction cone, (b) rectangular duct and turning diffuser with baffle	43
3.3 Centrifugal blower in Aerodynamic Lab, UTHM	44
3.4 Settling chamber with 4 units of mesh screen attached to the contraction cone	46
3.5 200 m long rectangular duct	48
3.6 Schematic diagram of the three-dimensional turning diffuser with preliminary airfoil baffle. All dimensions are not up to scale.	49
3.7 Three-dimensional turning diffuser with baffle made up of 3 mm acrylic plate	49
3.8 Schematic diagram of a Pitot static tube (Elyasi, 2009)	51
3.9 FLUKE 922 digital air flow meter and its function	52
3.10 Centre point of turning diffuser inlet, X_c	52
3.11 Pitot tube connection to digital manometer (Appendix C)	53
3.12 Pitot tube connected to digital manometer (left) and measurement of ΔP_{dyn} at point X_c at turning diffuser inlet (right)	53
3.13 (a) Pressure tapping at outlet and (b) inlet connected to digital Manometer using Triple-T piezometer tube	56
3.14 Basic concept of the 2D PIV system (Adrian, 2005)	58
3.15 PIV post processing and data analysis technique (Appendix D)	58
3.16 2D PIV setup	60
3.17 3D stereoscopic setup	61
3.18 Local outlet plane of interest points V_0 , V_1 , V_2 , V_3 and V_4	62
3.19 Pitot static reading at the outlet for validation with PIV values at V_0 and V_1	62
3.20 Medium density tracer particle seeding in PIV frame (Raffel et al., 2013)	63
3.21 Dantec F2010 Safex fog generator with remote control	64
3.22 Illumination parts from Dantec; (a) DualPower Laser screw-pumped cooling system, (b) Laser light guiding arm (c) Laser optic and (d) Nd:YAG Laser source	65
3.23 Calibration plate	67
3.24 Overlapping camera position for 3D stereoscopic setup	68

3.25	5 orientations of calibration plate for calibration in 3D stereoscopic PIV; (a) 20° incline to east side, (b) 20° incline to west side, (c) 20° incline to north side, (d) 20° incline to south side and (e) 0° flat position	68
3.26	Successful calibration (a) pinhole Image Model Fit (IMF) for 2D PIV and (b) Direct Linear Transform (DLT) for 3D PIV	69
3.27	Turning diffuser divided into 3 planes for 2D PIV setup	69
3.28	Masked area around turning diffuser for all planes in 2D PIV setup; (a) Plane 1, (b) Plane 2 and (c) Plane 3	71
3.29	Minor masked area around the outlet for 3D PIV setup from; (a) Camera 1 and (b) Camera 2	71
3.30	Vector flow in Plane 1 after image processing for 2D PIV setup	71
3.31	Vector statistic from (a) Camera 1 and (b) Camera 2 combined to produced (c) stereoscopic third velocity component contour, V_o	72
4.1	Extended CFD domain for three-dimensional (a) and two-dimensional (c) turning diffuser and actual geometry in experiment for three-dimensional (b) and two-dimensional (d) turning diffuser. All dimensions are in cm.	77
4.2	Turbulent flow boundary layer (ANSYS, 2010)	78
4.3	Value of y^+ in turbulent flow boundary layers (ANSYS, 2010)	78
4.4	Enhanced wall treatment in the sub-layer zone (ANSYS, 2010)	80
4.5	SIMPLE algorithm flow diagram (Versteeg & Malalasekera, 2007)	84
5.1	Schematic diagram of three-dimensional turning diffuser	90
5.2	(a) Airfoil parameters and (b) location of airfoil baffle in three-dimensional turning diffuser	92
5.3	(a) Plane 1 image location and (b) mask image with seeded particle flow	95
5.4	Point of X_c data acquisition to be compared with Pitot static probe reading and location of Line 1 at Plane 1	96
5.5	Flow structures on Plane 1 for all Re_{in} ; (a) 4.527E+04, (b) 5.110E+04, (c) 7.580E+04, (d) 9.950E+04 and (e) 1.263E+05	99
5.6	Velocity contour at Plane 1 extracted for all Re_{in} ; (a) 4.527E+04, (b) 5.110E+04, (c) 7.580E+04, (d) 9.950E+04 and (e) 1.263E+05.	101

5.7	Local inlet velocity, U_o plot along Line 1 together with U_{max} measured by Pitot static reading for comparison	102
5.8	(a) Original image location of Plane 2; (b) and (c) shows flow with seeded particle image containing reflections due to laser light sheet	103
5.9	Flow structure at Plane 2 for all Re_{in} tested; (a) 4.527E+04, (b) 5.110E+04, (c) 7.580E+04, (d) 9.950E+04 and (e) 1.263E+05	104
5.10	Velocity contour at Plane 2 for all Re_{in} tested; (a) 4.527E+04, (b) 5.110E+04, (c) 7.580E+04, (d) 9.950E+04 and (e) 1.263E+05	105
5.11	(a) Plane 3 desired location and (b) seeded flow after image masking	107
5.12	Flow structure at Plane 3 from 2D PIV setup for all Re_{in} tested; (a) 4.527E+04, (b) 5.110E+04, (c) 7.580E+04, (d) 9.950E+04 and (e) 1.263E+05	108
5.13	Flow structure comparison at $Re_{in}=4.527E+04$ between; (a) turning diffuser with baffle and (b) turning diffuser without baffle (Nordin et al., 2014a)	109
5.14	Flow structure comparison at $Re_{in}=1.263E+05$ between; (a) turning diffuser with baffle and (b) turning diffuser without baffle (Nordin et al., 2014a)	110
5.15	Both cameras mounted on traverse by using Scheimpflug rule facing outlet plane of interest	112
5.16	Points taken at the outlet for validation of Δt selection	112
5.17	Local third velocity component, V_o contour comparison between present study and previous study (Nordin et al., 2014a) for; $Re_{in}=4.527E+04$ ((a) and (c) respectively) and $Re_{in}=1.263E+05$ ((b) and (d) respectively).	115
5.18	Outlet plane of interest and allocated position of Line A and Line B	117
5.19	Local outlet velocities, V_o plotted graph along Line A; (a) present study, (b) Nordin et al. (2014a)	118
5.20	Local outlet velocities, V_o plotted graph along Line B; (a) present study, (b) Nordin et al. (2014a)	119
6.1	Two-dimensional turning diffuser with baffles computational domain	124
6.2	Two-dimensional turning diffuser with baffle constructed mesh with Enhanced Wall Treatment (EWT) function	125

6.3	Flow structures on Plane A for all Re_{in} ; (a) 4.527E+04, (b) 5.110E+04, (c) 7.580E+04, (d) 9.950E+04 and (e) 1.263E+05	128
6.4	Velocity contour on Plane A for all Re_{in} ; (a) 4.527E+04, (b) 5.110E+04, (c) 7.580E+04, (d) 9.950E+04 and (e) 1.263E+0	129
6.5	Three-dimensional turning diffuser with baffle computational domain	131
6.6	Three-dimensional turning diffuser with baffle constructed mesh with Enhanced Wall Treatment (EWT) function	132
6.7	Flow structure at Plane 1 for all Re_{in} ; (a) 4.527E+04, (b) 5.110E+04, (c) 7.580E+04, (d) 9.950E+04 and (e) 1.263E+0	133
6.8	Velocity contour at Plane 1 for all Re_{in} ; (a) 4.527E+04, (b) 5.110E+04, (c) 7.580E+04, (d) 9.950E+04 and (e) 1.263E+0	134
6.9	Flow structure at Plane 2 for all Re_{in} ; (a) 4.527E+04, (b) 5.110E+04, (c) 7.580E+04, (d) 9.950E+04 and (e) 1.263E+0	136
6.10	Velocity contour at Plane 2 for all Re_{in} ; (a) 4.527E+04, (b) 5.110E+04, (c) 7.580E+04, (d) 9.950E+04 and (e) 1.263E+0	137
6.11	Flow structure at Plane 3 for all Re_{in} ; (a) 4.527E+04, (b) 5.110E+04, (c) 7.580E+04, (d) 9.950E+04 and (e) 1.263E+0	139
6.12	Velocity contour at Plane 3 for all Re_{in} ; (a) 4.527E+04, (b) 5.110E+04, (c) 7.580E+04, (d) 9.950E+04 and (e) 1.263E+0	140
6.13	Velocity contour at outlet plane for all Re_{in} ; (a) 4.527E+04, (b) 5.110E+04, (c) 7.580E+04, (d) 9.950E+04 and (e) 1.263E+0	142
7.1	Mesh 1 unstructured grid for two-dimensional turning diffuser with baffles	145
7.2	Mesh 2 unstructured grid for two-dimensional turning diffuser with baffles	145
7.3	Mesh 3 unstructured grid for two-dimensional turning diffuser with baffles	146
7.4	Local outlet velocity, V_0 plotted along Line A for grid independent study test	147
7.5	Local outlet velocity, V_0 plotted along Line A for turbulence model test	148
7.6	Local outlet velocity, V_0 plotted along Line A for numerical scheme test	150
7.7	Local outlet velocity, V_0 plotted along Line A for convergence criteria test	151
7.8	Mesh 1 unstructured grid for three-dimensional turning diffuser with baffle	156

7.9	Mesh 2 unstructured grid for three dimensional turning diffuser with baffle	157
7.10	Mesh 3 unstructured grid for three-dimensional turning diffuser with baffle	157
7.11	Local outlet velocity, V_0 plotted along line A for grid independent study test	158
7.12	Local outlet velocity, V_0 plotted along line A for turbulence model test	159
7.13	Local outlet velocity, V_0 plotted along Line A for numerical scheme test	161
7.14	Local outlet velocity, V_0 plotted along Line A for convergence criteria test	162
8.1	(a) Location of the leading edge and separation point and (b) preliminary airfoil dimensions used in both the experiment and simulation	169
8.2	Flat plate baffle design in three-dimensional turning diffuser (all dimensions in cm); (a) side view and (b) isometric view	170
8.3	Flat plate baffle velocity contour at Plane A for all Re_{in} ; (a) $4.527E+04$, (b) $5.110E+04$, (c) $7.580E+04$, (d) $9.950E+04$ and (e) $1.263E+05$	174
8.4	Airfoil baffle velocity contour at Plane A for all Re_{in} ; (a) $4.527E+04$, (b) $5.110E+04$, (c) $7.580E+04$, (d) $9.950E+04$ and (e) $1.263E+05$	175
8.5	Location for plane of interest, Plane B	176
8.6	Flat plate baffle velocity contour at Plane B for all Re_{in} ; (a) $4.527E+04$, (b) $5.110E+04$, (c) $7.580E+04$, (d) $9.950E+04$ and (e) $1.263E+05$	177
8.7	Airfoil baffle velocity contour at Plane B for all Re_{in} ; (a) $4.527E+04$, (b) $5.110E+04$, (c) $7.580E+04$, (d) $9.950E+04$ and (e) $1.263E+05$	178
8.8	Local outlet velocity, V_0 plot along Line A comparison between flat plate and airfoil baffle for $Re_{in}=4.527E+04$ and $Re_{in}=1.263E+05$	180
8.9	Local outlet velocity, V_0 plot along Line B comparison between flat plate and airfoil baffle for $Re_{in}=4.527E+04$ and $Re_{in}=1.263E+05$	180
8.10	Allocated position of Line A, Line B and Line C	181

8.11	Local outlet velocity, V_o plot along Line C comparison between flat plate and airfoil baffle for $Re_{in}=4.527E+04$ and $Re_{in}=1.263E+05$	181
8.12	Velocity contour at outlet plane (flat plate baffle) for all Re_{in} ; (a) $4.527E+04$, (b) $5.110E+04$, (c) $7.580E+04$, (d) $9.950E+04$ and (e) $1.263E+05$	183
8.13	Different angle of attack tested in simulation	184
8.14	Location of data for C_{pa} plot around airfoil	187
8.15	C_{pa} plot around airfoil crossing z-axis=0	187
8.16	Velocity contour at Plane A for airfoil with; (a) AOA=11°, (b) AOA=14°, (c) AOA=17° (preliminary), (d) AOA=20° and (e) AOA=23°	189
8.17	Velocity contour at Plane B for airfoil with; (a) AOA=11°, (b) AOA=14°, (c) AOA=17° (preliminary), (d) AOA=20° and (e) AOA=23°	190
8.18	Outlet velocity contour at multiple positions for airfoil with AOA=23°	191
8.19	Outlet velocity contour at multiple positions for airfoil with AOA=20°	192
8.20	Outlet velocity contour at multiple positions for airfoil with AOA=17° (preliminary)	192
8.21	Different angle of attack tested in simulation	193
8.22	C_{pa} plot around airfoil across z-axis=0	196
8.23	Velocity contour at Plane B for airfoil with; (a) AOA=16°, (b) AOA=15°, (c) AOA=14°, (d) AOA=13° and (e) AOA=12°	197
8.24	Airfoil design with different t/c tested	199
8.25	C_{pa} plot around airfoil across z-axis=0	201
8.26	Velocity contour at Plane B; (a) Airfoil A, (b) Airfoil B, (c) Airfoil Base, (d) Airfoil C, (e) Airfoil D and (f) Airfoil E	203
8.27	Airfoil designs with different f/c tested	204
8.28	C_{pa} plot around airfoil across z-axis=0	207
8.29	Velocity contour at Plane B for; (a) Airfoil F, (b) Airfoil G, (c) Airfoil Base, (d) Airfoil H and (e) Airfoil I.	208
8.30	Airfoil designs with different chord length, c tested	209
8.31	C_{pa} plot around airfoil with different chord length, c	212
8.32	Velocity contour at Plane B for all airfoil; (a) Airfoil J, (b) Airfoil K, (c) Airfoil Base, (d) Airfoil L and (e) Airfoil M	213

LIST OF SYMBOLS

A	-	Current
A_1	-	Inlet area
A_2	-	Outlet area
c	-	Chord length
C_d	-	Drag coefficient
C_p	-	Turning diffuser pressure recovery coefficient
C_{pa}	-	Airfoil pressure coefficient
$C_{p_{ideal}}$	-	Pressure recovery for ideal turning diffuser
d	-	Spacing between vanes in cascade design
D_h	-	Hydraulic diameter
f/c	-	Camber-to-chord ratio
h_0	-	Spacing between vanes perpendicular to outflow direction
h_1	-	Spacing between vanes perpendicular to inflow direction
I	-	Turbulence intensity, %
K	-	Loss coefficient
k	-	Kinetic energy coefficient
L_{in}	-	Inner wall length
L_m	-	Centreline length
L_m/W_1	-	Centreline length to inlet width ratio
L_{out}	-	Outer wall length
N	-	Number of measurement points
P_{atm}	-	Atmospheric pressure = 101325 Pa
P_{gauge}	-	Gauge pressure
P_i	-	Inlet average static pressure
P_o	-	Outlet average static pressure

Re_{in}	-	Inlet Reynolds number
t	-	Airfoil thickness
f	-	Camber thickness
t/c	-	Thickness-to-chord ratio
U_{max}	-	Inlet maximum velocity
U_{in}	-	Inlet mean velocity
U_o	-	Inlet local velocity
V_o	-	Local outlet velocity
V_{out}	-	Mean outlet velocity
V_p	-	Particle velocity
ν	-	Air kinematic viscosity, 1.60E-05 m ² /s
\bar{c}_f	-	Skin friction coefficient
W_1	-	Inlet width
W_2	-	Outer width
ℓ_h	-	Hydrodynamic entrance length
y_p	-	First layer thickness
y^+	-	Size of grid cell nearest to the wall
σ_{out}	-	Outlet flow uniformity
η	-	Diffuser efficiency
ρ	-	Air density, 1.164 kg/m ³
μ	-	Air dynamic viscosity, 1.86E-05 kg/ms
λ	-	Laser wavelength
$\Delta\phi$	-	Turning angle
ε	-	Dissipation rate
ΔP_{dyn}	-	Dynamic pressure of moving fluid
Δx	-	Particle displacement between two consecutive images
Δt	-	Time between two light pulses

LIST OF ABBREVIATIONS

AR	- Area ratio
AOA	- Angle of attack
CAD	- Computer-aided Design
CCD	- Charge-coupled device
CDA	- Controlled diffusion concept
CFD	- Computational fluid dynamic
DEHS	- Di-Ethyl-Hexyl-Sabacar
DLT	- Direct linear transform
ES	- Evolution strategy
EVM	- Eddy viscosity model
EWT	- Enhanced Wall Treatment
HVAC	- Heating, Ventilation and Air Conditioning
IMF	- Image model fit
LES	- Large eddy simulation
MOGA	- Multi objective generic algorithm
Nd:YAG	- Neodym-yttrium-aluminium-garnet
OGV	- Outlet guide vanes
PIV	- Particle Image Velocimetry
RA	- Reattachment point
RANS	- Reynolds-averaged Navier-Stokes
RNG	- Renormalization group turbulence model
RPM	- Revolution per minute
RSM	- Reynolds stress model
S	- Separation point
SIMPLEC	- Semi-Implicit Method for Pressure-Linked Equation

SKE	- Standard K-Epsilon turbulence model
RKE	- Realizable K-Epsilon turbulence model
SST	- Shear stress transport model
UTHM	- Universiti Tun Huseein Onn Malaysia

LIST OF APPENDICES

APPENDIX	TITLE	PAGE
A	DEHS MSDS	231
B	Blower Manual	233
C	Digital Manometer Manual	235
D	PIV catalogue	239
E	3D traversing system specifications	240
F	Fog generator and fog fluid specifications	243
G	DualPower laser specifications	247
H	FlowSense 2M specifications	255
I	Turning diffuser with baffle detail design	257
J	Stereoscopic PIV contour	261
K	V_o along Line A, Line B and Line C	264

CHAPTER 1

INTRODUCTION

Investigation of flow patterns and flow characteristics for internal and external fluid flow has been of interest to researchers all around the world. The study of fluid mechanics deals with the action of forces on fluids, which in contrast to solids, can deform and flow under the action of shear stress. Such flows offer a lot of interesting topics to be discussed, especially when considering the vital role fluid mechanics plays in our everyday lives.

The diffuser, for an example, is one of the steady flow engineering devices introduced in fluid flow systems, which has the simplest design of an expanding area in the flow direction. By slowing down the flow and consequently resulting in the recovery of static pressure (Ghose, Datta, & Mukhopadhyay, 2013), following the conservation of energy, the diffuser's basic function is to convert kinetic energy into potential energy (Azad, 1996; Lee et al., 2013).

To minimize the weight and size of the engine, aviation gas turbine, for example, uses dump diffusers in the combustor (Ghose et al., 2013). On the other hand, in circulating fluidized bed application, as the lower section has a smaller cross-section as compared to the upper section, the diffuser is mounted, acting as a connector for both parts as shown in Figure 1.1 (Schut et al., 2000).

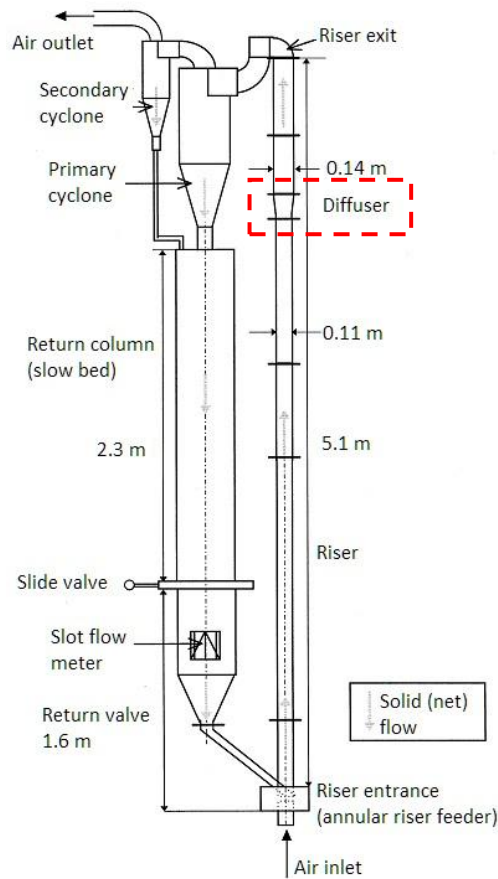


Figure 1.1: Schematic diagram of experimental circulating fluidised bed including diffuser (Schut et al., 2000)

Turning diffuser was favourable when involved with space restrictions applications (Gopaliya & Chaudhary, 2010). Intake ducts for aircraft engines use an S-shaped diffuser which also function as an interconnector between components in gas turbine engines (Mohamed, Djebedjian, & Rayan, 2000). In the heating, ventilation and air conditioning (HVAC) duct, the free discharge diffuser was used at the duct outlet system in order to reduce the air velocity when discharged into the atmosphere (Gan & Riffat, 1996) as shown in Figure 1.2. With a proper design compatibility test, both the bend and diffuser can be combined into a turning diffuser, especially when compactness is desired in the system.

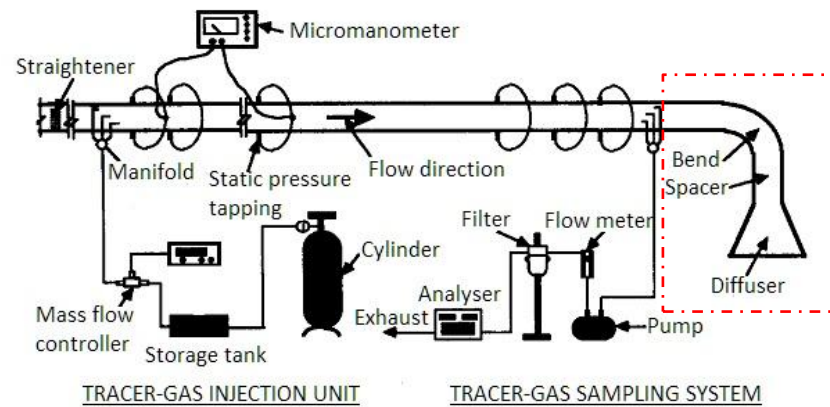


Figure 1.2: Test rig measurement of diffuser's pressure loss coefficient in HVAC free discharge duct system (Gan & Riffat, 1996)

The same concept was applied for the closed loop subsonic wind tunnel system. The diffuser in the closed loop wind tunnel was located downstream of the test section. In order to minimize loss of kinetic energy in the flow, the diffuser decelerates the flow after the test section (Calautit et al., 2014). As shown in Figure 1.3, the area covered by the closed loop subsonic wind tunnel can be reduced if both the 90° downstream turn and diffuser were combined into a turning diffuser.

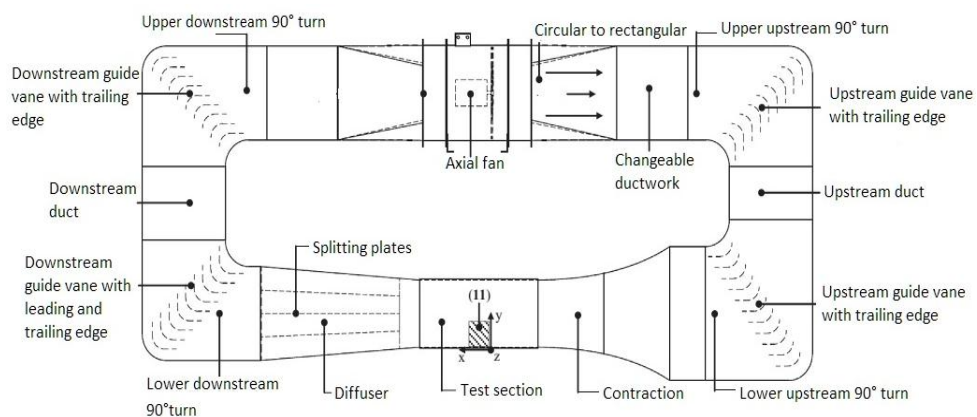


Figure 1.3: Closed loop subsonic wind tunnel detailed computer-aided design CAD model (Calautit et al., 2014)

1.1 Research background

There are two types of turning diffusers, namely the two-dimensional turning diffuser and the three-dimensional turning diffuser. Flow structure in the three-dimensional turning diffuser has been proven to be more distorted as compared to the two-dimensional turning diffuser (Nordin et al., 2014a). Consequently, higher pressure loss occurs in the three-dimensional turning diffuser due to curvature effects and diffusing activities. Both types of turning diffusers used in the present study closely resemble the turning diffuser used in a previous study (Chong, Joseph, & Davies, 2008; Nordin et al., 2014a)

The dimensions of the inlet surface area of a diffuser are denoted by W_1 and X_1 while the outlet dimensions are denoted by W_2 and X_2 . The two-dimensional turning diffuser has expanding cross-section in y-z plane where the length of X_1 and X_2 remain the same. Figure 1.4 and Figure 1.5 show the design of the two-dimensional turning diffuser and the three-dimensional turning diffuser.

On the other hand, the three-dimensional turning diffuser has different lengths for all W_1 , W_2 , X_1 , and X_2 . It has expanding cross section in both x-y and y-z planes. Due to this, the flow structure for the three-dimensional turning diffuser is much more complex to be investigated. Other than pressure recovery coefficient C_p , turning diffuser performance can be measured by calculating standard deviation of the outlet flow, σ_{out} . As a square root of variance in probability distribution (Othman, Wahab, & Raghavan, 2012), standard deviation represents variation of local outlet velocity, V_o to the mean outlet velocity, V_{out} .

Flow structure in turning diffuser is strongly dependent on turning angle ($\Delta\phi$), area ratio (AR), and inlet Reynolds number (Re_{in}). To avoid severe flow separation for both types of turning diffuser, 90° turning angle with AR=2.16 were selected as the optimum parameters of both turning diffusers in the present study (Nordin et al., 2012a, 2012b). As previous studies have proven the effects of varying inlet Reynolds number on turning diffuser performance in various applications (Djebdjian, 2001; Gopaliya & Chaudhary, 2010; Moonen et al., 2006), the present study on turning diffusers was operated within inlet Reynolds number range of $4.570E+04$ to $1.122E+05$, suitable for low subsonic wind tunnel and HVAC duct system applications.

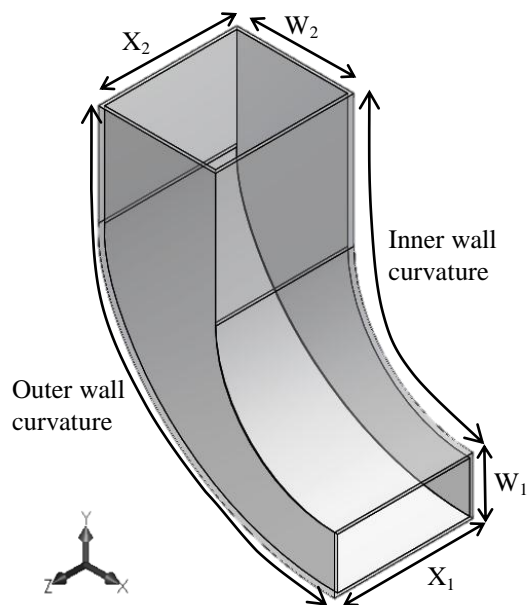


Figure 1.4: Design of the two-dimensional turning diffuser (Nordin et al., 2012)

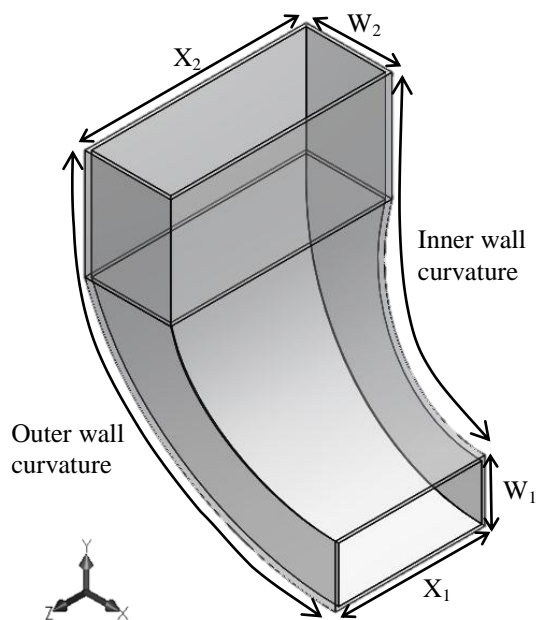


Figure 1.5: Design of the three-dimensional turning diffuser (Nordin et al., 2012)

1.2 Problem Statement

Secondary flow (flow separation) occurs mostly in diffuser applications. In circulating fluidized bed riser for example, flow separation leads to recirculation of gas and solids in the diffusers and consequently increases reflux ratio (Schut et al., 2000). In a dump diffuser, a recirculating vortex at the upper corner forms due to flow separation occurring at the outer wall (Ghose et al., 2013). Flow separation and reattachment in engineering situations are believed to contribute to pressure fluctuations, noise and also flow unsteadiness (Park & Sung, 1995).

Flow separation in a diffuser itself is unavoidable due to an adverse pressure gradient in diffuser flow (El-Askary & Nasr, 2009; Moonen et al., 2006; Wang et al., 2009). One of the approaches to reduce such losses in a diffuser is by installing guide vanes (baffles). In a closed loop wind tunnel, for example, in the upstream test section as shown in Figure 1.3 in Calautit et al. (2014), the diffuser was equipped with splitting plates and a 90° bend was installed with guide vanes. These are the approaches taken to reduce flow separation in both parts which can reduce the overall performance of the wind tunnel significantly.

For the two-dimensional 90° turning diffuser with AR=2.16, the approach for installing the baffle has been successfully investigated in a previous study (Noh@seth et al., 2013). By measuring the overall performance of the turning diffuser in terms of pressure recovery, C_p , and flow uniformity, σ_{out} , introduction of three units of flat plate baffles improved the overall performance by 50%. The present study will continue this effort by implementing a numerical approach to the same design of turning diffuser with baffle.

On the other hand, the three-dimensional turning diffuser can be more suitable for certain applications, even though it is proven to have a more complex and distorted flow as compared to the two-dimensional turning diffuser, which was highlighted in a previous study on the three-dimensional 90° turning diffuser with AR=2.16 conducted by Nordin et al. (2014a). The present study will continue the approach by installing the baffle to reduce flow separation, as well as improve the performance of the three-dimensional turning diffuser in terms of pressure recovery and flow uniformity.

It is essential to propose the optimum design of baffle for the three-dimensional turning diffuser application in order to improve its performance in terms of both pressure recovery and flow uniformity. Reducing flow separation will simultaneously reduce pressure fluctuations, noise and flow unsteadiness, as mentioned earlier, especially at the upstream section of turning diffuser in the application of closed loop low speed wind tunnel and HVAC duct system.

1.3 Objectives of study

The objectives of this study are:

1. To investigate the mechanism of flow structure in turning diffuser installed with baffle and studies the effects towards turning diffuser performance.
2. To propose an optimal design of baffles and evaluate the effectiveness of the new baffle design to improve turning diffuser performance.

1.4 Scope of study

The scope of this study covers;

1. A three-dimensional 90° turning diffuser with inlet dimension 13 cm × 5 cm and outlet dimension 19.5 cm × 7.2 cm, giving the area ratio of AR=2.16. The preliminary airfoil installed was optimized Wortmann FX60-100 taken from previous study (Sahlin et al., 1991).
2. The turning diffuser is preceded by a settling chamber and multiple screens, a contraction cone and long duct upstream, which adheres to the turbulent hydrodynamic length, to provide a fully developed flow at the turning diffuser inlet.

3. Inlet operating parameters, Re_{in} varied within the range of $4.527E+04$ (10 m/s) – $1.263E+05$ (28 m/s).
4. The turning diffuser performance is evaluated in terms of pressure recovery coefficient (C_p), which is measured through pressure tapping, and flow uniformity (σ_{out}), which is measured using Particle Image Velocimetry (PIV).
5. Simulations are done on both the two-dimensional and three-dimensional turning diffusers by using ANSYS Fluent. The K-Epsilon turbulence model and boundary conditions were verified and validated using experimental results.
6. The parametric study on the baffle design includes changes on; type of baffle between flat plate and airfoil, angle of attack, AOA ranging from 23° to 11° , thickness-to-chord ratio, t/c ranging from 5.35% to 13.27%, camber-to-chord ratio, f/c ranging from 7% to 13% and chord length, c ranging from 5 cm to 9 cm. Simulations on 23 designs of baffle include the performance comparison in terms of drag coefficient, C_d and airfoil pressure coefficient, C_{pa} profile.

1.5 Significance of study

The three-dimensional turning diffuser offers advantages in both applicability and compactness, especially in the HVAC duct system since many large buildings opt for centralized HVAC, which involves installation of the HVAC duct system. The current study focuses on designing new turning baffles to improve the performance of both the two-dimensional and three-dimensional turning diffuser with various inlet conditions. A number of previously available baffle designs are studied and evaluated in the attempt to propose a brand new baffle design with advantageous characteristics. Both experimental and numerical approaches are implemented for this purpose. An optimized baffle design will satisfy the need to achieve high-pressure recovery with less distortion of the outlet flow condition.

1.6 Thesis outline

The remainder of this thesis consists of another 8 chapters.

Chapter 2 presents a review on available literature to date referred to involving diffuser applications and theoretical background as well as development of experimental rig used in present study. Documentations on previous design of baffle which uses similar experimental setup was reviewed in order to propose preliminary airfoil to be installed in three-dimensional turning diffuser. Since present work involve both experimental and numerical approach, instrumentations on PIV sensors and techniques together with turbulence model used to study flow parameters were also reviewed.

Both Chapter 3 and Chapter 4 explain method and tools used in both experimental and numerical approach respectively. Chapter 3 starts with explanations on the overall experimental setup and later segregate each instrument in details. PIV measurement and instrumentation techniques were also discussed in details.

Chapter 4 continues with discussion on CFD modelling techniques which include mathematical model, computational domain, meshing, boundary conditions, solver algorithm and convergence criteria. Summarize input in ANSYS Fluent was also included in this chapter.

Chapter 5 laid out the experimental results from PIV, ranging from pressure recovery measurements data, flow structure from 2D and 3D PIV setup as well as measurement of turning diffuser outlet flow uniformity and efficiency. All data were compared to three-dimensional turning diffuser without baffle taken from previous study.

Chapter 6 continues with numerical results on velocity contour and flow structure for both two-dimensional turning diffuser and three-dimensional turning diffuser taking from ANSYS Fluent.

Chapter 7 focuses on validation and verification of the numerical analysis by using experimental data from Chapter 5. Verification of each CFD building block for both two-dimensional turning diffuser and three-dimensional turning diffuser numerical

analysis were discussed and the numerical results were validated with experimental results presented in Chapter 5.

Chapter 8 presents parametric study conducted on optimized Wortmann FX60-100 airfoil design including changes on design of baffle, AOA, t/c , f/c and chord length, c . After all parametric study conducted, the optimum design of baffle was proposed in this chapter.

Conclusions are drawn on the present research and contributions towards research society were made. Recommendation on future work was also included in the end of this thesis.

CHAPTER 2

LITERATURE REVIEW

In order to better comprehend most aspects in studying flow in both the two-dimensional and three-dimensional turning diffuser with baffle, a review of some concept and theoretical background on the experimental setup and numerical approach is quite essential. Included in this chapter is review on the basic industrial application of diffuser followed by development of the experimental rig used in the present study. The present study focuses more on improving turning diffuser performance by installing baffles. Thus, a review on various baffle designs from previous studies, taken from different cases, is included in this chapter. As mentioned in the previous chapter, turning diffuser outlet flow uniformity, σ_{out} was measured using PIV. Procedures on conducting the experiment using PIV by referring to other studies were also reviewed. Following the experimental procedures is a review on the numerical approach including validation and verification method conducted previously.

2.1 Diffuser applications and turning diffuser theoretical background

In general definition, diffusers are chambers that expand in flow direction, resulting in the decrease of fluid velocities along with increase of fluid pressure (Cermak, 1981). Industrial application, which uses the diffuser is either preceded by a bend or followed by a bend, includes a circulating fluidized bed riser, HVAC duct system as well as closed loop wind tunnel. Schematic experimental diagram of the circulating fluidized bed riser conducted by Schut et al.(2000) as shown in Figure 1.1 in the previous chapter is a clear example of diffuser application in duct system. The location of diffuser within the riser was varied as shown in Figure 2.1 and the effects on reflux ratio concludes that diffuser located 1050 cm below the exit provide better reflux ratio. Reflux ratio in parallel duct is higher when distance below the exit increases. Thus, proposing the use of turning diffuser in this case is rather inappropriate.

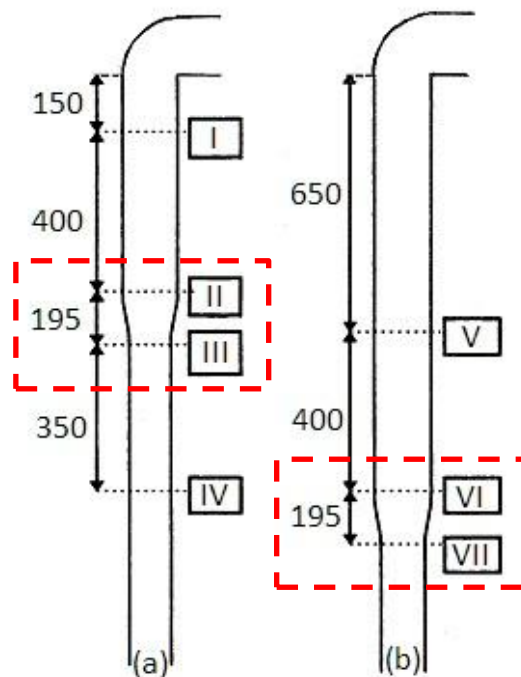


Figure 2.1: Two different positions of diffuser in the riser; (a) 550 cm below the exit and (b) 1050 cm below the exit (Schut et al., 2000)

In HVAC ductwork, free-discharge diffuser preceded by a bend was installed at the duct outlet to reduce the air velocity when discharge to atmosphere as part of room air distribution system. Gan and Riffat (1996) concluded in their study that a divergence angle smaller than 10° of pyramidal diffuser should be used to achieve flow regularity and stability discharged air, with the exception of spacer length of twice the hydraulic diameter, D_h ($2D_h$) should be introduced. El-Askary & Nasr (2009) concluded the same issue, where spacer length should be introduced between bend and diffuser which will contribute to loss reduction of the system. However, as shown in Figure 2.2, a highly distorted flow was still recorded. The turning diffuser could be proposed, together with installation of baffle to improve such flaws.

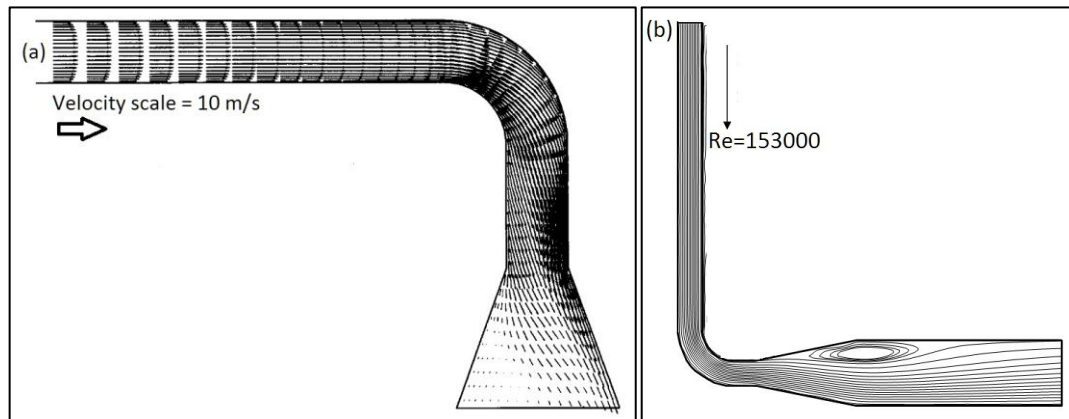


Figure 2.2: Bend-diffuser combination with short spacer shows highly distorted flow at diffuser exit for both studies by; (a) Gan & Riffat (1996), (b) El-Askary & Nasr (2009)

Diffusers are also commonly used in the wind tunnel system. Studies on subsonic close loop wind tunnel installed with principle components including the contraction cone, test section and diffuser has been conducted previously (Calautit et al., 2014; Gordon & Imbabi, 1998; Moonen, Blocken, & Carmeliet, 2007; Moonen et al., 2006). According to Moonen et al. (2006), flow separation will occur in several sections; entrance and exit of test section, 180° turn and sudden change in cross-sectional area. For the wind tunnel, the main aerodynamic objective is to make sure the flow is steady throughout the test section and has uniform speed (Calautit et al.,

2014). A closed loop wind tunnel has four 90° turn as shown in Figure 1.3 in previous chapter.

For the 90° upstream turn (Section 4), guide vanes were installed to reduce flow separation, whereas for 90° lower upstream turn (Section 8), guide vanes were mounted to direct the flow to be parallel to test section centre line. At the same time, it helped improved flow uniformity just before entering contraction cone. Both 90° turn downstream and upstream of the diffuser's outlet were also installed with guide vanes, with the same objective to reduce flow separation occurring in the turn (Calautit et al., 2014). As shown in Figure 2.3, significant improvement on velocity contour in closed loop wind tunnel concluded that guide vanes installed in diffuser and 90° turn helps reduce flow separation and improve flow uniformity entering the test section.

However, when space limitations were the factor to be considered in building a closed loop wind tunnel, diffusing and turning activities could be combined as a turning diffuser. Other terms for turning diffuser used in previous studies were expanding corner, diffusing bend and curved diffuser. Studies on turning diffusers were previously conducted, and they highlighted a few subjects to be brought up for discussion (Chong et al., 2008; Djebedjian, 2001; McMillan, 1982; Majumdar et al., 1996, 1998, 1999; Sinha et al., 2010, 2011, 2012).

Flow structure in a curved diffuser depends greatly on centreline length to inlet width ratio (L_m/W_I), area ratio (AR), inlet condition (Re_{in}) and turning angle ($\Delta\phi$). Furthermore, higher shear strains near convex curved wall flow structure were initiated when higher inlet Reynolds numbers were introduced (Djebedjian, 2001). According to Chong et al. (2008), centrifugal forces were introduced in curved ducts, which cause deflected core flow to the outer wall and consequently due to adverse pressure gradient reduce the velocity at the outer wall.

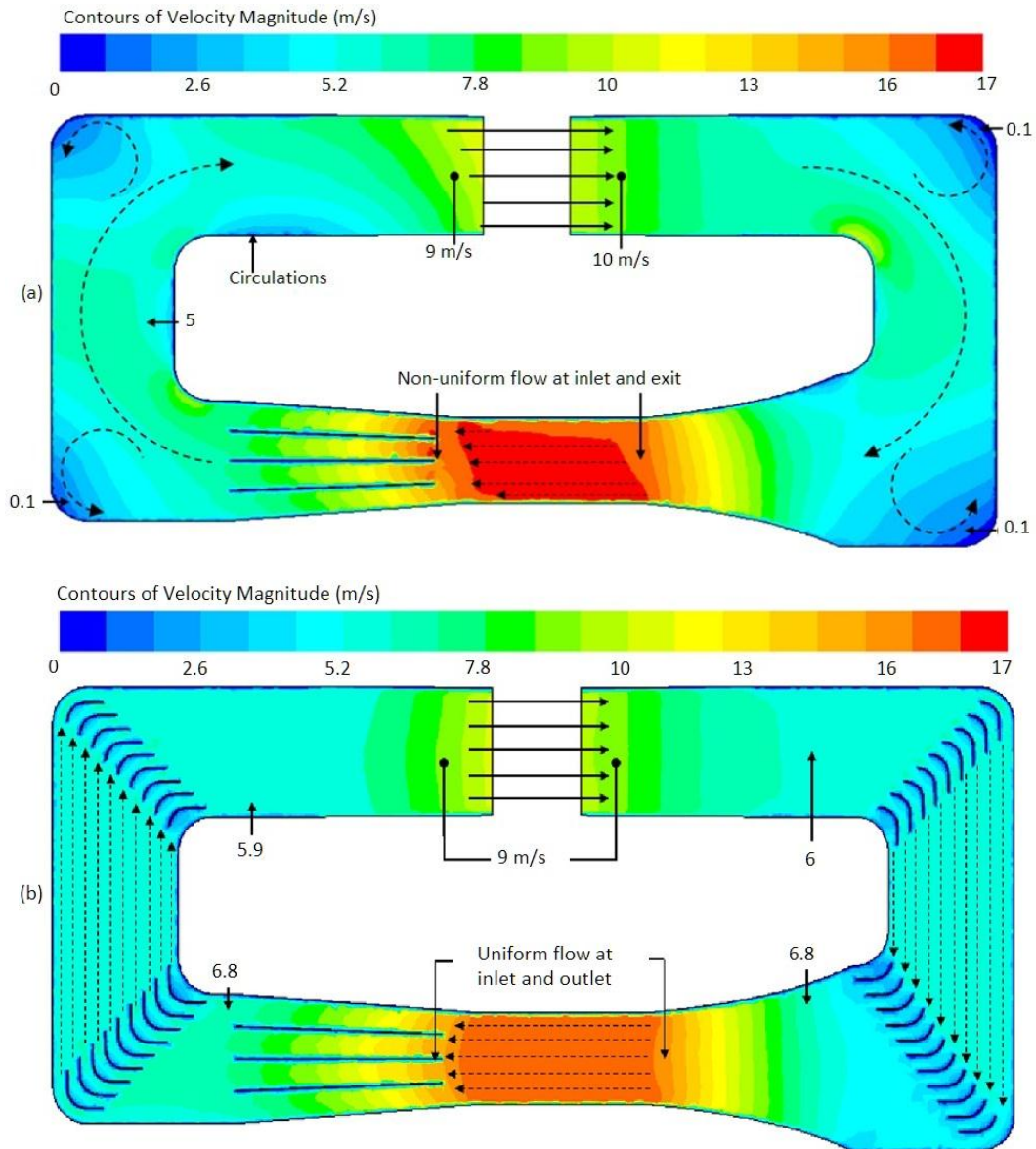


Figure 2.3: (a) Contours of velocity magnitude for wind tunnel before and (b) after installation of guide vanes (Calautit et al., 2014)

Majumdar et al. (1996, 1998, and 1999) in all their studies experimentally investigated 90° curved diffuser as well as 180° curved diffuser flow characteristics. Severe flow distortion was observed due to centrifugal force created by the curvature wall. Efforts were done to improve flow characteristic in the curved diffuser was by installing vanes. Other than 90° and 180° curved diffuser, small divergence angle curved diffuser such as 30° , 37.5° and 42° curved annular diffuser were previously studied (Sinha et al., 2010, 2011 and 2012) all resulting in high velocity flow

accumulated and shifted towards the outer (concave) wall especially at the outlet of curved diffuser.

All these studies highlighted critical flow separation due to curvature effects as well as diffusing activities in curved diffuser. Secondary flow cannot be neglected since it contributes to losses in the system. Efforts can be done in improving flow characteristics in curved diffuser, since it offers wide industrial applications especially in restricted space cases. Next section will outline a review on previous research focusing on the two-dimensional and three-dimensional rectangular cross section turning diffuser together with development of experimental rig used in present study.

2.2 Experimental rig development on low subsonic wind tunnel feature

Nordin et al. (2011) started research on performance of a bend-diffuser with baffles installed which was measured and compared to a bend-diffuser without baffles. The tested diffuser has an area ratio (AR) of 7.2 with 13 cm \times 13 cm square inlet and axial length of 49 cm. Three locations were chosen to be measured, i.e., before bend (S1), before diffuser (S2) and after diffuser (S3) with two planes (A and B) each using Pitot static probe and digital manometer with accuracy of ± 0.1 Pa. Macbain's (MacBain, 2003) patent was selected as baffle design to be adopted in the experiment. Details are shown in Figure 2.4 and Figure 2.5. It was proven that with the installation of baffles in bend-diffuser system, the overall performance improved in terms of pressure loss reduction. As shown in Table 2.1, loss coefficient (K) was reduced for almost all cases except inside the diffuser. This is due to excessive separation in the diffuser itself.

After seeing a promising improvement in overall losses for bend-diffuser, Nordin et al. (2012a) proceed by adopting a turning diffuser in replace of bend-diffuser. A numerical approach was conducted by varying turning diffuser geometric conditions (AR=1.6, 2.0 and 3.0) and operating parameters (Re_{in} ranging from 23 to 2.123E+05). Simulations on each case were conducted using 3 different turbulence

models, which was Standard K-Epsilon turbulence model (SKE), the Shear Stress Transport model (SST K-Omega) and the Reynolds Stress Model (RSM).

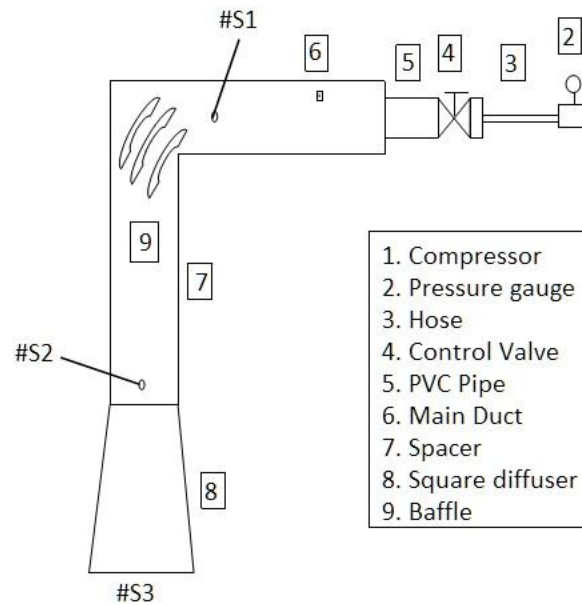


Figure 2.4: Location chosen for measurement; S1, S2, S3 (Nordin et al., 2011)

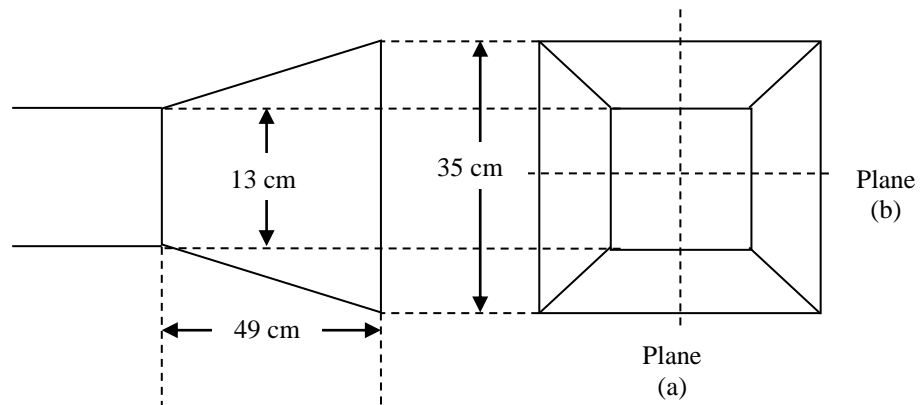


Figure 2.5: Two planes selected for each location measurement (Nordin et al., 2011)

Table 2.1: Pressure loss coefficient (K) (Nordin et al., 2011)

Part	Loss Coefficient (K)	
	Without baffles	With Baffles
Bend (a)	1.249	0.227
Bend (b)	1.145	-0.351
Diffuser (a)	1.290	2.899
Diffuser (b)	0.578	1.275
System (a)	1.306	0.573
System (b)	1.746	-0.134

Turning diffuser performances were measured in terms of pressure recovery (C_p) and outlet's flow uniformity (σ_{out}). Higher value of C_p represents high pressure recovery, whereas lower value of σ_{out} represents high flow uniformity. From the simulation at specific Re_{in} , pressure recovery increases with increasing AR. Conversely, flow uniformity decreases with increasing Re_{in} . On the other hand, at specific AR, while pressure recovery increase with increasing Re_{in} , flow uniformity decrease with increasing Re_{in} . After all, the increase of AR yields smaller effects on the flow uniformity as compared to the effects by increasing Re_{in} .

Thus, Nordin et al. (2012a) carried out more intensive studies on varying Re_{in} to find its effects on the flow uniformity. Consequently, an optimum geometric configuration of turning diffuser was proposed; AR=1.6 running at $Re_{in}=2.653E+04$, which corresponded to performance value of $C_p=0.320$ and $\sigma_{out}=1.620$. However, results between simulation and experimental data deviates up to 34.1%, concluding that further improvement on the existing rig need to be implemented.

Nordin et al. (2013) then developed a low subsonic wind tunnel for turning diffuser application to ensure flow at the inlet of turning diffuser need to be steady, uniform and fully developed. Even sufficient hydrodynamic entrance length was introduced, poor joining of duct and abrupt change of cross sectional area between the blower and the duct might be the cause of 34.1% deviation between the numerical and experimental results in previous study (Nordin et al., 2012a). Several improvements were done to the system as shown in Figure 2.6.

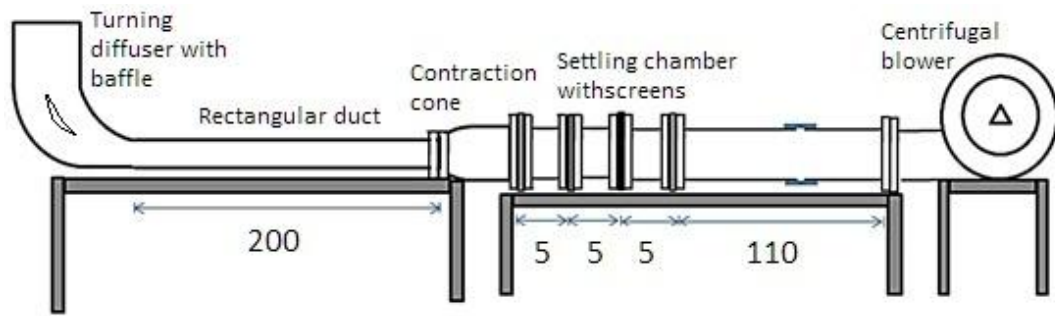


Figure 2.6: Rig development of low subsonic wind tunnel. All dimensions in cm. (Nordin et al., 2013)

To develop steady flow, a centrifugal blower with 3-phase inverter controller was used. Settling chamber and multiple screens made of metal wire interwoven were installed to improve the mean flow uniformity and reduce oncoming turbulence. The contraction cone will help to accelerate flow from the settling chamber, and it is expected to have steady, uniform and free separation out-going flow. Hydrodynamic length was introduced earlier on before connected to the turning diffuser's inlet. Thus, at the turning diffuser's inlet, the flow is believed to be steady, uniform and fully developed.

Nordin et al. (2014b) then verified the fully developed flow entering turning diffuser using Pitot static probe at 5 different points. Flow entering the turning diffuser was proved to be fully developed based on the velocity profile which resembles the boundary layer of a turbulent fully developed flow as shown in Figure 2.7. The outlet local velocity was also obtained using Particle Image Velocimetry (PIV) at 5 different points. Small average differences of 0.8%-1.2% between PIV result and Pitot static probe offered promising PIV measurement and rig implementation.

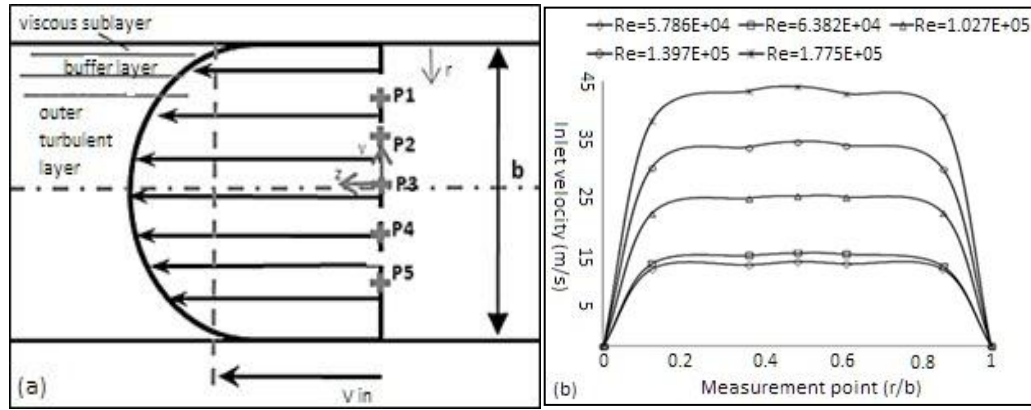


Figure 2.7: (a) Five points location at inlet for measurements of fully developed flow and (b) velocity profile measured using Pitot static probe (Nordin et al., 2014b)

After a strong verification of the rig and the whole system, Nordin et al. (2014a) continues the experimental investigation on two-dimensional turning diffuser by varying inflow Reynolds number. Pressure recovery was measured using pressure tapping at both inlet and outlet of the turning diffuser connected via triple-T piezometer and measured using a digital Manometer, whereas the outlet flow uniformity was measured using PIV.

5 different values of outlet flow velocity were measured. Verification of PIV result was obtained by comparing manual measurement of the local outlet velocity, V_o using Pitot static probe with PIV measurement. Table 2.2 shows the deviation between both approaches. These outputs were used by Noh@Seth et al. (2013) as reference in the study of improving flow uniformity and pressure recovery of the two-dimensional turning diffuser by means of installing baffles.

Table 2.2: C_p measured for each Re_{in} tested and verification of PIV results for two-dimensional turning diffuser (Nordin et al., 2014a)

Re_{in}	C_p	V_o Pitot	V_o PIV	Deviation (%)
5.786E+04	0.191	4.98	4.92	1.2
6.382E+04	0.209	5.92	5.87	0.8
1.027E+05	0.216	11.05	10.64	3.7
1.397E+05	0.221	15.45	15.34	0.7
1.775E+05	0.239	19.75	19.05	3.5

Noh@Seth et al. (2013) continued the effort to improve flow uniformity and pressure recovery by installing flat plate baffles. 3 units of flat plate baffles were designed, acting as a small turning diffuser in the existing turning diffuser in order to avoid flow abruption. Figure 2.8 shows the design of flat plate baffles in two-dimensional turning diffuser.

Using the same experimental rig, an improvement of 54.6% on pressure recovery was proven after installing the two-dimensional turning diffuser with baffles. Best produced pressure recovery of $C_p=0.526$ was recorded as compared to $C_p=0.239$ for two-dimensional turning diffuser without baffle at the highest Reynolds number tested. As for the flow uniformity, the best σ_{out} was $\sigma_{out}=3.235$ at the highest Reynolds number tested, with an improvement of 47.1%. Table 2.3 shows the resulting output from the experiment done by Noh@Seth et al. (2013).

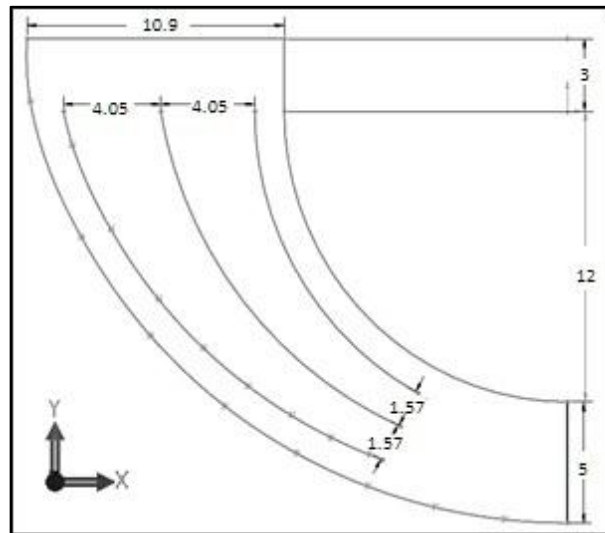


Figure 2.8: Flat plate baffle designed by Noh@Seth et al. (2013). All dimensions in cm.

Table 2.3: Result comparison between Noh@Seth et al. (2013) and Nordin et al. (2014a) for both C_p and σ_{out}

Re_{in}	σ_{out} (Noh@seth et al., 2013)	σ_{out} (Nordin et al., 2014a)	Improvement (%)
5.786E+04	0.719	1.755	58.864
6.382E+04	0.683	1.852	63.032
1.027E+05	2.437	2.910	16.240
1.397E+05	2.621	4.947	46.492
1.775E+05	3.235	6.128	47.127

Re_{in}	C_p (Noh@seth et al., 2013)	C_p (Nordin et al., 2014a)	Improvement (%)
5.786E+04	0.413	0.191	53.849
6.382E+04	0.418	0.209	50.100
1.027E+05	0.433	0.216	50.225
1.397E+05	0.491	0.221	55.035
1.775E+05	0.526	0.239	54.625

Other than flow uniformity (σ_{out}), velocity contour at the outlet produced by PIV was also compared. Noh@Seth et al. (2013) successfully improve and direct the deflected flow more towards the inner wall as compared to Nordin et al. (2014a). For reference, Figure 2.9 shows velocity contour with flow vector comparison for the highest Re_{in} tested in both experiments. In other words, flow separation at the inner wall region has been successfully reduced by installing baffle which correlate with smaller value of σ_{out} measured.

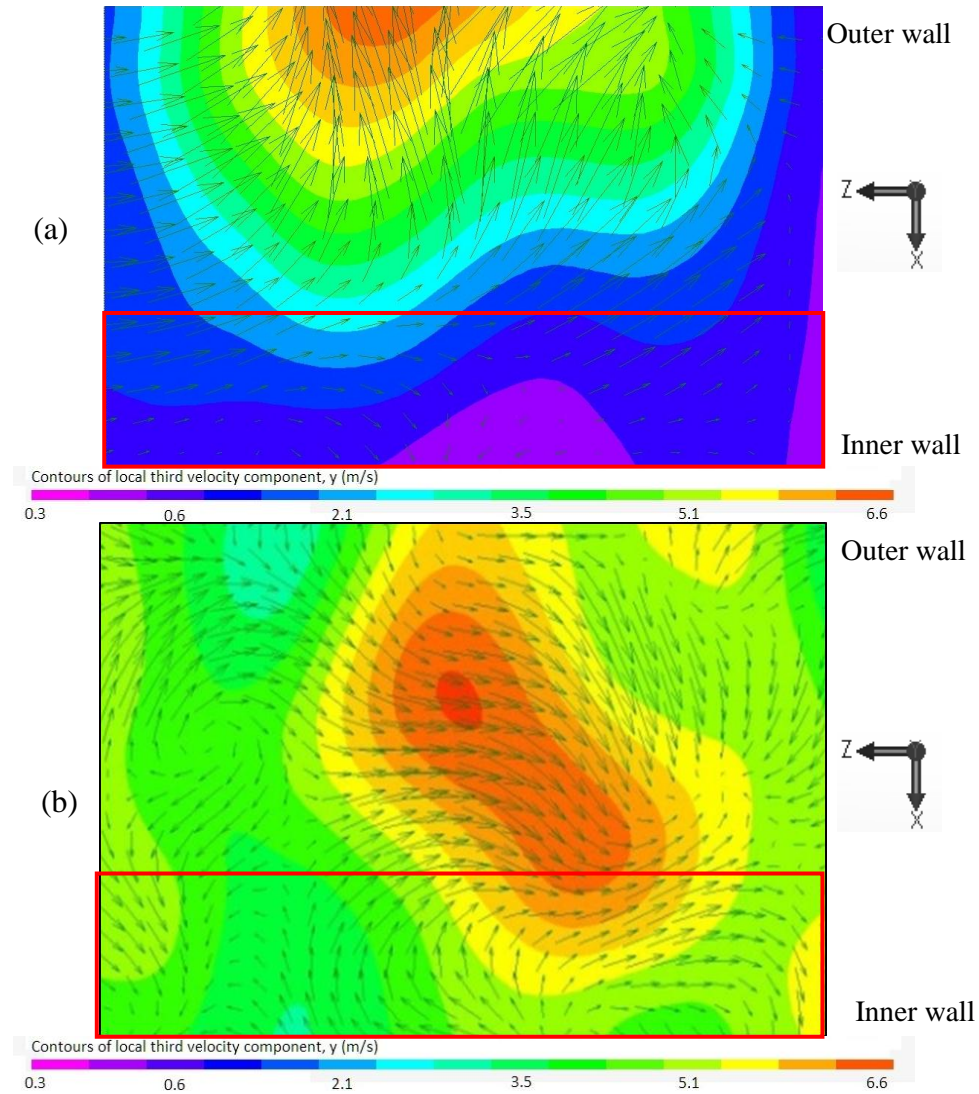


Figure 2.9: Outlet velocity contour and vector comparison between (a) Nordin et al. (2014a) and (b) Noh@Seth et al. (2013). Red box indicates inner wall region.

Study on turning diffuser can be widely enhanced to various dimensions of turning diffuser. Since the two-dimensional turning diffuser offered extensive improvement on replacing bend-diffuser, especially with the installation of baffle, Nordin et al. (2012b) extended their studies by varying the area ratios of the three-dimensional turning diffuser. Generally, the three-dimensional turning diffuser has more complex flow as compared to the two-dimensional turning diffuser as prescribed in previous chapter; hence offer wider discussion on flow characteristics and turning diffuser performance.

Nordin et al. (2012b) investigated three different cases; the two-dimensional turning diffuser (Case A), three-dimensional turning diffuser with $AR=2.0$ (Case B)

and three-dimensional turning diffuser with $AR=4.0$ (Case C). All cases were compared and concluded that pressure recovery and flow uniformity for Case B is lower than Case A, due to more complex flow and diffusing activities for three-dimensional turning diffuser.

Latest research done by Nordin et al. (2014a) was on the performance of the three-dimensional turning diffuser at various inlet conditions as compared to the two-dimensional turning diffuser by using similar experimental setup and rig. Table 2.4 and 2.5 shows the comparison of both experiments. The research proposed for inflow $Re_{in}=1.027E+05-1.775E+05$, the three-dimensional turning diffuser is more reliable and as for $Re_{in}=5.786E+04-6.382E+04$, the two-dimensional turning diffuser is much more favourable. This is only if flow uniformity is of interest to subject. On the other hand, if pressure recovery is becoming the concern, the three-dimensional turning diffuser performed better within $Re_{in}=5.786E+04-6.382E+04$ and $Re_{in}=1.027E+05-1.775E+05$ for the two-dimensional turning diffuser.

Table 2.4: Mean outlet velocity, V_{out} and flow uniformity comparison, σ_{out} (Nordin et al., 2014a)

Re_{in}	2-D Turning Diffuser		3-D Turning Diffuser	
	V_{out} (m/s)	σ_{out} (m/s)	V_{out} (m/s)	σ_{out} (m/s)
5.786E+04	1.57	1.75	2.07	1.82
6.382E+04	1.61	1.85	2.62	2.25
1.027E+05	2.31	2.91	3.03	2.7
1.397E+05	4.85	4.90	5.68	4.64
1.775E+05	5.75	6.12	5.95	5.05

Table 2.5: Pressure recovery, C_p comparison (Nordin et al., 2014a)

Re_{in}	2-D Turning Diffuser	3-D Turning Diffuser
	C_p	C_p
5.786E+04	0.191	0.210
6.382E+04	0.209	0.217
1.027E+05	0.216	0.203
1.397E+05	0.221	0.219
1.775E+05	0.239	0.194

REFERENCES

- Abdulmouti, H., & Mansour, T. M. (2006). The technique of PIV and its applications. In *10th International Congress on Liquid Atomization and Spray Systems*, Kyoto, Japan.
- Abe, K. I., & Ohya, Y. (2004). An investigation of flow fields around flanged diffusers using CFD. *Journal of wind engineering and industrial aerodynamics*, 92(3), 315-330.
- Abe, K., Nishida, M., Sakurai, A., Ohya, Y., Kihara, H., Wada, E., & Sato, K. (2005). Experimental and numerical investigations of flow fields behind a small wind turbine with a flanged diffuser. *Journal of Wind Engineering and Industrial Aerodynamics*, 93(12), 951-970.
- Adebayo, D. S., (2012) *Annular flows and their interaction with a cylindrical probe*. University of Leicester. Ph.D. Thesis.
- Adrian, R. J. (2005). Twenty years of particle image velocimetry. *Experiments in fluids*, 39(2), 159-169.
- Ahmed, N., (2013) Design features of a low turbulence return circuit subsonic wind tunnel having interchangeable test sections. In: Ahmed, N. A. (Ed). *Wind Tunnel-Designs and Their Diverse Engineering Applications*. Croatia: InTech. pp. 29-57.
- Aider, J. L., Beaudoin, J. F., & Wesfreid, J. E. (2010). Drag and lift reduction of a 3D bluff-body using active vortex generators. *Experiments in fluids*, 48(5), 771-789.
- Ariff, M., Salim, S. M., & Cheah, S. C. (2009). Wall y^+ approach for dealing with turbulent flow over a surface mounted cube: part 1—low Reynolds number. In *Proceedings of the 7th International Conference on CFD in the Minerals and Process Industries*, Melbourne, Australia (pp. 9-11).

- Azad, R. S. (1996). Turbulent flow in a conical diffuser: a review. *Experimental Thermal and Fluid Science*, 13(4), 318-337.
- Azzola, J., Humphrey, J. A. C., Iacovides, H., & Launder, B. E. (1986). Developing turbulent flow in a U-bend of circular cross-section: measurement and computation. *Journal of fluids engineering*, 108(2), 214-221.
- Bell, J. H. and Mehta, R. D., Boundary-layer predictions for small low-speed contractions. *American Institute of Aeronautics and Astronautics Journal*. 1989. 27(3): 372-374.
- Birch, N. (1984). *The calculation of 3D flow in curved ducts using Q385*. Rolls-Royce Theoretical Sciences Group, Derby. Report TSG0161.
- Blechinger, C. J. (1971). *The influence of inlet velocity distribution on the flow through a plane curved diffuser*. Iowa State University, Ph.D. Thesis.
- Blevins, R. D. (1984). *Applied fluid dynamics handbook*. New York, Van Nostrand Reinhold Co.
- Calautit, J. K., Chaudhry, H. N., Hughes, B. R., & Ghani, S. A. (2013). Comparison between evaporative cooling and a heat pipe assisted thermal loop for a commercial wind tower in hot and dry climatic conditions. *Applied Energy*, 101, 740-755.
- Calautit, J. K., Chaudhry, H. N., Hughes, B. R., & Sim, L. F. (2014). A validated design methodology for a closed-loop subsonic wind tunnel. *Journal of Wind Engineering and Industrial Aerodynamics*, 125, 180-194.
- Cermak, J. E. (1981). Wind tunnel design for physical modeling of atmospheric boundary layers. *Journal of the American Society of Civil Engineers*, 107, 623-642.
- Chang, S. M., Humphrey, J. A. C., & Modavi, A. (1983). Turbulent-flow in a strongly curved u-bend and downstream tangent of square cross-sections. *PhysicoChemical Hydrodynamics*, 4(3), 243-269.
- Chaudhry, H. N., Calautit, J. K., Hughes, B. R., & Sim, L. F. (2015). CFD and experimental study on the effect of progressive heating on fluid flow inside a thermal wind tunnel. *Computation*, 3(4), 509-527.
- Choi, Y. D., Iacovides, H., & Launder, B. E. (1989). Numerical computation of turbulent flow in a square-sectioned 180 deg bend. *Journal of Fluids Engineering*, 111(1), 59-68.

- Chong, T. P., Joseph, P. F., & Davies, P. O. (2008). A parametric study of passive flow control for a short, high area ratio 90deg curved diffuser. *Journal of Fluids Engineering*, 130(11), 111104-1-12.
- Corsiglia, V. R., Olson, L. E. and Falarski, M. D., (1984) *Aerodynamic characteristics of the 40-by 80/80- by 120-foot wind tunnel at NASA Ames Research Center*. NASA Technical Memorandum 85946.
- Dixon, S. L. (1998), *Fluid Mechanics, Thermodynamics of Turbomachinery*. 4th Ed. New York. McGraw-Hill.
- Djebedjian, B. (2001). Numerical and experimental investigations of turbulent flow in a 180° curved diffuser. In *ASME Division of Fluid Dynamics Summer Meeting*.
- El-Askary, W. A., & Nasr, M. (2009). Performance of a bend–diffuser system: Experimental and numerical studies. *Computers & Fluids*, 38(1), 160-170.
- Elyasi, S., (2009) *Development of UV photoreactor models for water treatment*. University of British Columbia. Ph.D. Thesis.
- Farsimadan, E., & Mokhtarzadeh-Dehghan, M. R. (2010). An experimental study of the turbulence quantities in the boundary layer and near-wake of an airfoil placed at upstream of a 90° bend. *Experimental Thermal and Fluid Science*, 34(8), 979-991.
- Friedman, D., & Westphal, W. R. (1952). *Experimental investigation of a 90 cascade diffusing bend with an area ratio of 1.45: 1 and with several inlet boundary layers*. NACA Tech. Note, 2668.
- Fukumasu, N. K., Guenther, C. K. F. and Yanagihara, J. I., (2013) PIV analyses of the influence on flow structure of vane design in swirl type air diffusers. 8th *World Conference on Experimental Heat Transfer, Fluid Mechanics and Thermodynamics*. June 16-20. Lisbon, Portugal. 2013.
- Gan, G., & Riffat, S. B. (1996). Measurement and computational fluid dynamics prediction of diffuser pressure-loss coefficient. *Applied energy*, 54(2), 181-195.
- Gan, L., (2012) Stereoscopic PIV and its applications on reconstruction three-dimensional flow field. in Cavazzini, G., *Characteristics, Limits and Possible Applications*. INTECH Open Access Publisher.

- Gartmann, A., Fister, W., Schwanghart, W., & Müller, M. D. (2011). CFD modelling and validation of measured wind field data in a portable wind tunnel. *Aeolian Research*, 3(3), 315-325.
- Gelder, T. F., Moore, R. D., Sanz, J. M. and Mcfarland, E. R., (1985) *Wind tunnel turning vanes of modern design*. Lewis Research Center, Cleveland, Ohio. NASA Technical Memorandum AIAA-86-0044.
- Ghorbanian, K., Soltani, M. R., & Manshadi, M. D. (2011). Experimental investigation on turbulence intensity reduction in subsonic wind tunnels. *Aerospace science and Technology*, 15(2), 137-147.
- Ghose, P., Datta, A., & Mukhopadhyay, A. (2013). Effect of dome shape on static pressure recovery in a dump diffuser at different inlet swirl. *International Journal of Emerging Technology and Advanced Engineering*, 3, 465-471.
- Gopaliya, M. K., Goel, P., Prashar, S., & Dutt, A. (2011). CFD analysis of performance characteristics of S-shaped diffusers with combined horizontal and vertical offsets. *Computers & Fluids*, 40(1), 280-290.
- Gordon, R., & Imbabi, M. S. (1998). CFD simulation and experimental validation of a new closed circuit wind/water tunnel design. *Journal of fluids engineering*, 120(2), 311-318.
- Versteeg, H. K. and Malalasekera, W., (2007) “*An introduction to computational fluid dynamic the finite volume method*”, 2nd Edition, Pearson Education Limited.
- Hu, H., Saga, T., Kobayashi, T., Okamoto, K., & Taniguchi, N. (1998). Evaluation of the cross correlation method by using PIV standard images. *Journal of Visualization*, 1(1), 87-94.
- Jakirlić, S., Kadavelil, G., Kornhaas, M., Schäfer, M., Sternel, D. C., & Tropea, C. (2010). Numerical and physical aspects in LES and hybrid LES/RANS of turbulent flow separation in a 3-D diffuser. *International Journal of Heat and Fluid Flow*, 31(5), 820-832.
- Johl, G. S., (2010) *The design and performance of a 1.9m x 1.3m indraft wind tunnel*. Loughborough University. Ph.D. Thesis.
- Johl, G., Passmore, M. and Render, P., (2007) Design and performance of thin, circular arc wind-tunnel turning vanes. *The Aeronautical Journal*. 111(1116): 115-118.

- Johnson, R. W., (1984) *Turbulent convecting flow in a square duct with a 180° bend*. University of Manchester. Ph.D. Thesis.
- Jung, W. J., Affes, H., Perng, C. Y., & Chu, D. (1998). A Preliminary Study on Curvature Effect Turbulence Modeling for Ducted and Turbomachinery Flows & Wall Treatment. In *Proceedings, FEDSM*, 98(1998), pp. 21-25.
- Kim, H. J., Lee, S., & Fujisawa, N. (2006). Computation of unsteady flow and aerodynamic noise of NACA0018 airfoil using large-eddy simulation. *International journal of heat and fluid flow*, 27(2), 229-242.
- Kim, J., Moin, P., & Moser, R. (1987). Turbulence statistics in fully developed channel flow at low Reynolds number. *Journal of fluid mechanics*, 177, 133-166.
- Kishore, R. A., & Priya, S. (2013). Design and experimental verification of a high efficiency small wind energy portable turbine (SWEPT). *Journal of Wind Engineering and Industrial Aerodynamics*, 118, 12-19.
- Koch, H., Kozulovic, D., & Hoeger, M. (2012). Outlet Guide Vane Airfoil for Low Pressure Turbine Configurations. *AIAA Paper*, (2012-2979).
- Kozak, J. D., (2000) *Investigation of inlet guide vane wakes in a F109 turbofan engine with and without flow*. Virginia Polytechnic Institute and State University. Ph.D Thesis.
- Lastra, M. R., Oro, J. M. F., Vega, M. G., Marigorta, E. B., & Morros, C. S. (2013). Novel design and experimental validation of a contraction nozzle for aerodynamic measurements in a subsonic wind tunnel. *Journal of Wind Engineering and Industrial Aerodynamics*, 118, 35-43.
- Lee, G. G., Allan, W. D., & Boulama, K. G. (2013). Flow and performance characteristics of an Allison 250 gas turbine S-shaped diffuser: effects of geometry variations. *International Journal of Heat and Fluid Flow*, 42, 151-163.
- Lien, K., Monty, J. P., Chong, M. S., & Ooi, A. (2004, November). The entrance length for fully developed turbulent channel flow. In *15th Australian Fluid Mechanics Conference*, 15, pp. 356-363.
- Lindgren, B., & Johansson, A. V. (2002). Design and evaluation of a low-speed wind-tunnel with expanding corners. *Department of Mechanics, KTH, Report No. TRITA-MEK, 14*.

- Lindgren, B., Österlund, J., & Johansson, A. V. (1998). Measurement and calculation of guide vane performance in expanding bends for wind-tunnels. *Experiments in fluids*, 24(3), 265-272.
- Liu, Y., & Liaw, B. (2009). Drop-weight impact tests and finite element modeling of cast acrylic/aluminum plates. *Polymer Testing*, 28(8), 808-823.
- MacBain, S. M. (2003). *U.S. Patent No. 6,668,580*. Washington, DC: U.S. Patent and Trademark Office.
- Majumdar, B., Mohan, R., Singh, S. N., & Agrawal, D. P. (1998). Experimental study of flow in a high aspect ratio 90 deg curved diffuser. *Journal of fluids engineering*, 120(1), 83-89.
- Majumdar, B., Singh, S. N., & Agrawal, D. P. (1996). Flow characteristics in a large area ratio curved diffuser. *Proceedings of the Institution of Mechanical Engineers, Part G: Journal of Aerospace Engineering*, 210(1), 65-75.
- Majumdar, B., Singh, S. N., & Agrawal, D. P. (1999). Flow structure in a 180 degrees curved diffusing duct. *Arabian Journal for Science and Engineering*, 24(1 B), 79-87.
- Mathes, A. R., (1997) *Experimental analysis of an advanced-design, quasi-radial diffuser receiving an oscillating jet*. Virginia Polytechnic Institute and State University. Msc. Thesis.
- Mathew, J., (2006) *Design, fabrication and characterization of an anechoic wind tunnel facility*. University of Florida. Ph.D. Thesis.
- McMillan, O. J., (1982) *Mean-flow measurements of the flow field diffusing bend*. NASA contractor report 3634.
- Medina, R., Motamedi, A., Okcay, M., Uygur Oztekin, B., Menezes, G. B., & Pacheco-Vega, A.J. (2012). On the implementation of open source CFD system to flow visualization in fluid mechanics. In *American Society for Engineering Education*. American Society for Engineering Education.
- Mehta, R. D., & Bell, J. H. (1989). Boundary-layer predictions for small low-speed contractions. *AIAA journal*, 27(3), 372-374.
- Melling, A. (1997). Tracer particles and seeding for particle image velocimetry. *Measurement Science and Technology*, 8(12), 1406.
- Miller, D. S., (1978) *Internal Flow System*. 1st Edition. Houston. Gulf Publishing Company.

- Modi, P. P., & Jayanti, S. (2004). Pressure losses and flow maldistribution in ducts with sharp bends. *Chemical Engineering Research and Design*, 82(3), 321-331.
- Mohamed, S. M., Djebedjian, B., & Rayan, M. M. (2000). Experimental and numerical studies of flow in a logarithmic spiral curved diffuser. In *Proceedings, FEDSM '2000, ASME Fluids Engineering Summer Meeting Conference*. Boston. pp. 1-8.
- Moonen, P., Blocken, B., & Carmeliet, J. (2007). Indicators for the evaluation of wind tunnel test section flow quality and application to a numerical closed-circuit wind tunnel. *Journal of Wind Engineering and Industrial Aerodynamics*, 95(9), 1289-1314.
- Moonen, P., Blocken, B., Roels, S., & Carmeliet, J. (2006). Numerical modeling of the flow conditions in a closed-circuit low-speed wind tunnel. *Journal of Wind Engineering and Industrial Aerodynamics*, 94(10), 699-723.
- Moore, C. A. and Kline, S. J., (1958) *Some effects of vanes and of turbulence in two-dimensional wide angle subsonic diffuser*. NACA. TN-4080.
- Morel, T. (1975). Comprehensive design of axisymmetric wind tunnel contractions. *Journal of Fluids Engineering*, 97(2), 225-233.
- Münch, C., & Métais, O. (2006). Large Eddy Simulations of the turbulent flow in curved ducts: influence of the curvature radius. In *Direct and Large-Eddy Simulation VI* (pp. 209-216). Springer Netherlands.
- Myong, H. K. (1997). New parameters describing extra straining effects in turbulence models. *Journal of fluids engineering*, 119(3), 721-724.
- Nakano, T., Fujisawa, N., Oguma, Y., Takagi, Y., & Lee, S. (2007). Experimental study on flow and noise characteristics of NACA0018 airfoil. *Journal of Wind Engineering and Industrial Aerodynamics*, 95(7), 511-531.
- Nguyen, V. T., Nestmann, F., & Eisenhauer, N. (2000). Numerical computation of turbulent flow in different curved rectangular-sectioned channels. In *Proceedings, FEDSM'00, 2000 ASME Fluids Engineering Division Summer Meeting*, pp. 11-15.
- Noh@Seth, N. H., Nordin, N., Othman, S., & Raghavan, V. R. (2014). Investigation of flow uniformity and pressure recovery in a turning diffuser by means of baffles. In *Applied Mechanics and Materials*, 465, pp. 526-530.

- Nordin, N., Othman, S., R Raghavan, V., Mohideen Batcha, M. F., & Idris, S. M. (2011). Experimental investigation of pressure losses and flow characteristics in bend-diffusers by means of installing turning baffles. *2nd International Conference of Mechanical Engineering*, Putrajaya, Kuala Lumpur.
- Nordin, N., Karim, A., Ambri, Z., Othman, S., & Raghavan, V. R. (2012). Design and development of low subsonic wind tunnel for turning diffuser application. In *Advanced Materials Research*, 614, pp. 586-591.
- Nordin, N., Othman, S., R Raghavan, V., Karim, A., & Ambri, Z. (2012). Verification of 3-D stereoscopic PIV operation and procedures. *International Journal of Engineering & Technology IJET-IJENS*, 12(4), 19-26.
- Nordin, N., R Raghavan, V., Othman, S., Karim, A., & Ambri, Z. (2012). Compatibility of 3-D turning diffusers by means of varying area ratios and outlet-inlet configurations. *ARPJ Journal of Engineering and Applied Sciences*, 7(6), 708-713.
- Nordin, N., Raghavan, V. R., Othman, S., Karim, A., & Ambri, Z. (2012). Numerical investigation of turning diffuser performance by varying geometric and operating parameters. *Applied Mechanics and Materials*, 229, pp. 2086-2093.
- Nordin, N., Abdul Karim, Z. A., Othman, S. and Raghavan, V. R., (2014). Verification of fully developed flow entering diffuser and particle image velocimetry procedures. *Applied Mechanics and Materials*. 465-466: 1352-1356.
- Nordin, N., Karim, A., Ambri, Z., Othman, S., & Raghavan, V. R. (2014). The performance of turning diffusers at various inlet conditions. *Applied Mechanics and Materials*, 465, pp. 597-602.
- ANSYS (2010). *Introduction to ANSYS FLUENT : Turbulence Modelling*. ANSYS Customer Training Material.
- Oberkampf, W. L., & Trucano, T. G. (2002). Verification and validation in computational fluid dynamics. *Progress in Aerospace Sciences*, 38(3), 209-272..
- Othman, S., Wahab, A. A., & Raghavan, V. R. (2010). Statistical analysis on the design of flow modifying centre-bodies in a plenum chamber. *CFD Letters*, 1(2), 78-86.

- Park, T. S. and Sung, H. J., (1995) A nonlinear low-Reynolds-number k - ϵ model for turbulent separated and reattaching flows. *International Journal of Heat Mass Transfer*. 38(14): 2657-2666.
- Parsons, D. J., & Hill, P. G. (1973). Effects of curvature on two-dimensional diffuser flow. *Journal of Fluids Engineering*, 95(3), 349-360.
- Prasad, A. K. (2000). Stereoscopic particle image velocimetry. *Experiments in fluids*, 29(2), 103-116.
- Raffel, M., Willert, C., Wereley, S. & Kompenhans, J. (2007). *Particle image velocimetry: A practical guide*. 2nd Edition. Berlin. Springer.
- Rhee, G. H., & Sung, H. J. (1996). A nonlinear low-Reynolds-number k - ϵ model for turbulent separated and reattaching flows—II. Thermal field computations. *International journal of heat and mass transfer*, 39(16), 3465-3474.
- Rojas, J., Whitelaw, J. H., & Yianneskis, M. (1984). Flow in sigmoid diffusers of moderate curvature. In *4th Symposium on Turbulent Shear Flows* (Vol. 1, p. 6).
- Sagi, C. J., & Johnston, J. P. (1967). The Design and Performance of Two-Dimensional, Curved Diffusers: Part I—Exposition of Method and Part II—Experiment, Evaluation of Method, and Conclusions. *Journal of Basic Engineering*, 89(4), 715-731.
- Şahin, B., Ward-Smith, A. J., & Lane, D. (1995). The pressure drop and flow characteristics of wide-angle screened diffusers of large area ratio. *Journal of wind engineering and industrial aerodynamics*, 58(1), 33-50.
- Sahlin, A., & Johansson, A. V. (1991). Design of guide vanes for minimizing the pressure loss in sharp bends. *Physics of Fluids A: Fluid Dynamics (1989-1993)*, 3(8), 1934-1940.
- Sajanikar, M. B., Kar, S., & Powle, U. S. (1982). Experimental investigation of incompressible flow in curved diffusers. In *Proceedings of Eleventh National Conference on Fluid Mechanics and Fluid Power*, Hyderabad, India.
- Schreiber, H. A., Steinert, W., Sonoda, T., & Arima, T. (2003). Advanced high turning compressor airfoils for low Reynolds number condition: Part 2—Experimental and numerical analysis. In *ASME Turbo Expo 2003, collocated with the 2003 International Joint Power Generation Conference*. pp. 451-463.

- Schut, S. B., Van Der Meer, E. H., Davidson, J. F., & Thorpe, R. B. (2000). Gas–solids flow in the diffuser of a circulating fluidised bed riser. *Powder Technology*, 111(1), 94-103.
- Senthil, K. S., Sankar, G. M., Kamalakannan, K., Santhana, B. K., & Yogesh, P. M. (2011). Design and computational analysis of NACA 846A110 and NACA 837A110 airfoils. In *Aerospace Conference, 2011 IEEE* (pp. 1-9). IEEE.
- Shah, A. I., Normah, M. G., Jamaluddin, M. S., Aminullah, A. R. M., & Dairobi, G. A. (2011). Stack geometry effects on flow pattern with particle Image Velocimetry (PIV). *Jurnal Mekanikal*, (33), 82-88.
- Shahin, I., Gadala, M., Alqaradawi, M., & Badr, O. (2013). Three dimensional computational study for spiral dry gas seal with constant groove depth and different tapered grooves. *Procedia Engineering*, 68, 205-212.
- Siddique, S. A., Design, development and CFD validation of a subsonic wind tunnel. University of Michigan. Unpublished.
- Sinha, P. K., & Majumdar, B. (2011). Numerical investigation of flow through annular curved diffusing duct. *International Journal of Engineering & Technology IJET-IJENS*, 3(03), 190-196.
- Sinha, P. K., Mullick, A. N., Halder, B., & Majumdar, B. (2010). A parametric investigation of flow through an annular curved diffuser. *Journal of International Review of Aerospace Engineering*, 3(5), 249-256.
- Sinha, P. K., Mullick, A. N., Halder, B., & Majumdar, B. (2011). Computational analysis of flow performance in a c-shape subsonic diffuser. *International Journal of Engineering Research and Applications*, 1(3), 824-829.
- Song, C. C. S. and Wetzel, J. M., (1988) *Physical and mathematical modelling of the HYKAT*. University of Minnesota, Minnesota. Project report No.282.
- Standard, A. I. A. A. (1999). *Assessment of experimental uncertainty with application to wind tunnel testing*. Washington DC. AIAA S-017A.
- Stewart, J. N., Wang, Q., Moseley, R. P., Bearman, P. W., & Harvey, J. K. (1996). Measurement of vortical flows in a low speed wind tunnel using particle image velocimetry. In *Proc. 8th Int. Symp. on Applications of Laser Techniques to Fluid Mechanics*, Lisbon.
- Tsikata, J. M., & Tachie, M. F. (2013). Adverse pressure gradient turbulent flows over rough walls. *International Journal of Heat and Fluid Flow*, 39, 127-145.

- Velázquez-Araque, L., Mendoza Pérez, L. D., & Nožička, J. (2014). Analysis of air flow past and through the 2415-3S airfoil for an unmanned aerial vehicle with internal propulsion system. *Journal of Systemics, Cybernetics and Informatics*, 12(4), 26-31.
- Wang, Y. C., Hsu, J. C., Kuo, P. C., & Lee, Y. C. (2009). Loss characteristics and flow rectification property of diffuser valves for micropump applications. *International Journal of Heat and Mass Transfer*, 52(1), 328-336.
- White, F. M., (2008) *Fluid Mechanics*. 4th edition. McGraw-Hill.
- Willert, C., Raffel, M., Kompenhans, J., Stasicki, B., & Kähler, C. (1996). Recent applications of particle image velocimetry in aerodynamic research. *Flow Measurement and Instrumentation*, 7(3), 247-256.
- Winter, K. G., (1952) *Comparative test of thick and thin turning vanes in the royal aircraft establishment 4 x 3-ft wind tunnel*. Aeronautical Research Council Reports and Memoranda. A.R.C Technical Report.
- Yaras, M. I., & Orsi, P. (2004). Measurements of the transient velocity field in a strongly curved diffusing bend with periodic inflow unsteadiness. *Experiments in fluids*, 36(2), 363-372.
- Yin, J. F., & Yu, S. Z. (1993). Investigation of turbulent separation-reattachment flow in a curved-wall diffuser. *International journal of heat and fluid flow*, 14(2), 129-137.
- Young, D. F., Munson, B. R. and Okiishi, T. H., (2004) *A brief introduction to fluid mechanics*. 3rd edition. New Jersey, USA. John Wiley & Sons.